10. Nogee, L. M., de Mello, D. E., Dehner, L. P., and Colten, H. R. (1993) *N. Engl. J. Med.* **328,** 406–410
11. Nogee, L. M., Dunbar, A. E., III, Wert, S. E., Askin, F., Hamvas, A., and Whitsett, J. A. (2001) *N. Engl. J. Med.* **344,** 573–579
12. Shulenin, S., Nogee, L. M., Annilo, T., Wert, S. E., Whitsett, J. A., and Dean, M. (2004) *N. Engl. J. Med.* **350,** 1296–1303
13. Hawgood, S., Derrick, M., and Poulain, F. (1998) *Biochim. Biophys. Acta* **1408,** 150–160
14. Whitsett, J. A., and Weaver, T. E. (2002) *N. Engl. J. Med.* **347,** 2141–2148
15. deMello, D. E., Nogee, L. M., Heyman, S., Krous, H. F., Hussain, M., Merritt, T. A., Hsueh, W., Haas, J. E., Heidelberger, K., Schumacher, R., and Colten, H. R. (1994) *J. Pediatr.* **125,** 43–50
16. Beers, M. F., and Mulugeta, S. (2005) *Annu. Rev. Physiol.* **67,** 663–696
17. Horowitz, A. D., Baatz, J. E., and Whitsett, J. A. (1993) *Biochemistry* **32,** 9513–9523
18. Glasser, S. W., Burhans, M. S., Korfhagen, T. R., Na, C. L., Sly, P. D., Ross, G. F., Ikegami, M., and Whitsett, J. A. (2001) *Proc. Natl. Acad. Sci. U. S. A.* **98,** 6366–6371
19. Cheong, N., Madesh, M., Gonzales, L. W., Zhao, M., Yu, K., Ballard, P. L., and Shuman, H. (2006) *J. Biol. Chem.* **281,** 9791–9800
20. Thomas, A. Q., Lane, K., Phillips, J., III, Prince, M., Markin, C., Speer, M., Schwartz, D. A., Gaddipati, R., Marney, A., Johnson, J., Roberts, R., Haines, J., Stahlman, M., and Loyd, J. E. (2002) *Am. J. Respir. Crit. Care Med.* **165,** 1322–1328
21. Yamano, G., Funahashi, H., Kawanami, O., Zhao, L. X., Ban, N., Uchida, Y., Morohoshi, T., Ogawa, J., Shioda, S., and Inagaki, N. (2001) *FEBS Lett.* **508,** 221–225
22. Mulugeta, S., Gray, J. M., Notarfrancesco, K. L., Gonzales, L. W., Koval, M., Feinstein, S. I., Ballard, P. L., Fisher, A. B., and Shuman, H. (2002) *J. Biol. Chem.* **277,** 22147–22155
23. Yoshida, I., Ban, N., and Inagaki, N. (2004) *Biochem. Biophys. Res. Commun.* **323,** 547–555
24. Bullard, J. E., Wert, S. E., Whitsett, J. A., Dean, M., and Nogee, L. M. (2005) *Am. J. Respir. Crit. Care Med.* **172,** 1026–1031
25. Niwa, H., Yamamura, K., and Miyazaki, J. (1991) *Gene (Amst.)* **108,** 193–199
26. Nagata, K., Yamamoto, A., Ban, N., Tanaka, A. R., Matsuo, M., Kioka, N., Inagaki, N., and Ueda, K. (2004) *Biochem. Biophys. Res. Commun.* **324,** 262–268
27. Matsuo, M., Kioka, N., Amachi, T., and Ueda, K. (1999) *J. Biol. Chem.* **274,** 37479–37482
28. Matsuo, M., Tanabe, K., Kioka, N., Amachi, T., and Ueda, K. (2000) *J. Biol. Chem.* **275,** 28757–28763
29. Voorhout, W. F., Veenendaal, T., Haagsman, H. P., Weaver, T. E., Whitsett, J. A., van Golde, L. M., and Geuze, H. J. (1992) *Am. J. Physiol.* **263,** L479–L486
30. Wang, W. J., Russo, S. J., Mulugeta, S., and Beers, M. F. (2002) *J. Biol. Chem.* **277,** 19929–19937
31. Higgins, C. F., and Linton, K. J. (2004) *Nat. Struct. Mol. Biol.* **11,** 918–926
32. McGuffin, L. J., Bryson, K., and Jones, D. T. (2000) *Bioinformatics (Oxf.)* **16,** 404–405
33. Chen, J., Lu, G., Lin, J., Davidson, A. L., and Quiocho, F. A. (2003) *Mol. Cell* **12,** 651–661
34. Locher, K. P., Lee, A. T., and Rees, D. C. (2002) *Science* **296,** 1091–1098
35. Schwede, T., Kopp, J., Guex, N., and Peitsch, M. C. (2003) *Nucleic Acids Res.* **31,** 3381–3385
36. Tanaka, A. R., Abe-Dohmae, S., Ohnishi, T., Aoki, R., Morinaga, G., Okuhira, K., Ikeda, Y., Kano, F., Matsuo, M., Kioka, N., Amachi, T., Murata, M., Yokoyama, S., and Ueda, K. (2003) *J. Biol. Chem.* **278,** 8815–8819
37. Jensen, T. J., Loo, M. A., Pind, S., Williams, D. B., Goldberg, A. L., and Riordan, J. R. (1995) *Cell* **83,** 129–135
38. Wang, X., Matteson, J., An, Y., Moyer, B., Yoo, J. S., Bannykh, S., Wilson, I. A., Riordan, J. R., and Balch, W. E. (2004) *J. Cell Biol.* **167,** 65–74
39. Prevelige, P., Jr., and Fasman, G. (1989) in *Prediction of Protein Structure and the Principles of Protein Conformation* (Fasman, G., ed) pp. 391–416, Plenum Publishing Corp., New York
40. Davidson, A. L., and Chen, J. (2004) *Annu. Rev. Biochem.* **73,** 241–268
41. Situ, D., Haimeur, A., Conseil, G., Sparks, K. E., Zhang, D., Deeley, R. G., and Cole, S. P. (2004) *J. Biol. Chem.* **279,** 38871–38880
42. Eilers, M., Shekar, S. C., Shieh, T., Smith, S. O., and Fleming, P. J. (2000) *Proc. Natl. Acad. Sci. U. S. A.* **97,** 5796–5801
43. Zhang, D. W., Gu, H. M., Vasa, M., Muredda, M., Cole, S. P., and Deeley, R. G. (2003) *Biochemistry* **42,** 9989–10000
44. Rivera, A., White, K., Stohr, H., Steiner, K., Hemmrich, N., Grimm, T., Jurklies, B., Lorenz, B., Scholl, H. P., Apfelstedt-Sylla, E., and Weber, B. H. (2002) *Am. J. Hum. Genet.* **67,** 800–813
45. Fumagalli, A., Ferrari, M., Soriani, N., Gessi, A., Foglieni, B., Martina, E., Manitto, M. P., Brancato, R., Dean, M., Allikmets, R., and Cremonesi, L. (2001) *Hum. Genet.* **109,** 326–338
46. Allikmets, R., Singh, N., Sun, H., Shroyer, N. F., Hutchinson, A., Chidambaram, A., Gerrard, B., Baird, L., Stauffer, D., Peiffer, A., Rattner, A., Smallwood, P., Li, Y., Anderson, K. L., Lewis, R. A., Nathans, J., Leppert, M., Dean, M., and Lupski, J. R. (1997) *Nat. Genet.* **15,** 236–246
47. Lewis, R. A., Shroyer, N. F., Singh, N., Allikmets, R., Hutchinson, A., Li, Y., Lupski, J. R., Leppert, M., and Dean, M. (1999) *Am. J. Hum. Genet.* **64,** 422–434
48. des Georges, M., Guittard, C., Altieri, J. P., Templin, C., Sarles, J., Sarda, P., and Claustres, M. (2004) *J. Cyst. Fibros.* **3,** 265–272
49. Vankeerberghen, A., Wei, L., Jaspers, M., Cassiman, J. J., Nilius, B., and Cuppens, H. (1998) *Hum. Mol. Genet.* **7,** 1761–1769
50. Dork, T., Dworniczak, B., Aulehla-Scholz, C., Wieczorek, D., Bohm, I., Mayerova, A., Seydewitz, H. H., Nieschlag, E., Meschede, D., Horst, J., Pander, H. J., Sperling, H., Ratjen, F., Passarge, E., Schmidtke, J., and Stuhrmann, M. (1997) *Hum. Genet.* **100,** 365–377
51. Colonna, M., Bresnahan, M., Bahram, S., Strominger, J. L., and Spies, T. (1992) *Proc. Natl. Acad. Sci. U. S. A.* **89,** 3932–3936

A T3587G germ-line mutation of the *MDR1* gene encodes a nonfunctional P-glycoprotein

Kazuyoshi Mutoh,[1] Junko Mitsuhashi,[1,2] Yasuhisa Kimura,[7] Satomi Tsukahara,[2] Etsuko Ishikawa,[2] Kimie Sai,[3,4] Shogo Ozawa,[3,5] Jun-ichi Sawada,[3,6] Kazumitsu Ueda,[7] Kazuhiro Katayama,[1] and Yoshikazu Sugimoto[1,2]

[1]Department of Chemotherapy, Kyoritsu University of Pharmacy; [2]Division of Gene Therapy, Cancer Chemotherapy Center, Japanese Foundation for Cancer Research; [3]Project Team for Pharmacogenetics and Divisions of [4]Xenobiotic Metabolism and Disposition, [5]Pharmacology, and [6]Biochemistry and Immunochemistry, National Institute of Health Sciences, Tokyo, Japan and [7]Laboratory of Biochemistry, Division of Applied Life Sciences, Graduate School of Agriculture, Kyoto University, Kyoto, Japan

Abstract

The human *multidrug resistance gene 1* (*MDR1*) encodes a plasma membrane P-glycoprotein (P-gp) that functions as an efflux pump for various structurally unrelated anticancer agents. We have identified two nonsynonymous germ-line mutations of the *MDR1* gene, C3583T *MDR1* and T3587G *MDR1*, in peripheral blood cell samples from Japanese cancer patients. Two patients carried the C3583T *MDR1* allele that encodes H1195Y P-gp, whereas a further two carried T3587G *MDR1* that encodes I1196S P-gp. Murine NIH3T3 cells were transfected with pCAL-MDR-IRES-ZEO constructs carrying either wild-type (WT), C3583T, or T3587G *MDR1* cDNA and selected with zeocin. The resulting zeocin-resistant mixed populations of transfected cells were designated as 3T3/WT, 3T3/H1195Y, and 3T3/I1196S, respectively. The cell surface expression of I1196S P-gp in 3T3/I1196S cells could not be detected by fluorescence-activated cell sorting, although low expression of I1196S P-gp was found by Western blotting. H1195Y P-gp expression levels in 3T3/H1195Y cells were slightly lower than the corresponding WT P-gp levels in 3T3/WT cells. By immunoblotting analysis, both WT P-gp and H1195Y P-gp were detectable as a 145-kDa protein, whereas I1196S P-gp was visualized as a 140-kDa protein. 3T3/I1196S cells did not show any drug resistance unlike 3T3/H1195Y cells. Moreover, a vanadate-trap assay showed that the I1196S P-gp species lacks ATP-binding activity. Taken together, we conclude from these data that T3587G *MDR1* expresses a nonfunctional P-gp and this is therefore the first description of such a germ-line mutation. We contend that the T3587G *MDR1* mutation may affect the pharmacokinetics of *MDR1*-related anticancer agents in patients carrying this allele. [Mol Cancer Ther 2006; 5(4):877–84]

Introduction

P-glycoprotein (P-gp), also known as ABCB1, is a 170- to 180-kDa transmembrane glycoprotein that functions as an efflux pump for various structurally unrelated anticancer drugs, such as the *Vinca* alkaloids, anthracyclines, and taxanes (1–4). P-gp is expressed in a variety of normal human tissues and cells, such as the small and large intestine, adrenal gland, kidney, liver, placenta, and the capillary endothelial cells of the brain and testes (5, 6). P-gp also mediates the excretion of its substrates from the intestine and therefore inhibits their intestinal absorption (7). In addition, P-gp mediates the biliary excretion and renal tubular secretion of its substrates (8, 9). Moreover, the coadministration of P-gp substrate anticancer agents and P-gp inhibitors, such as verapamil, increases both the plasma concentration and the area under the concentration-time curve of these substrate agents (10, 11). Mice lacking *multidrug resistance gene 1* (*MDR1*)–type P-gps (*mdr1a/mdr1b−/−* mice) display large changes in the pharmacokinetics of digoxin and other drugs (12, 13). Hence, the low expression of P-gp in normal cells/tissues alters the pharmacokinetics of its substrate anticancer agents.

Recently, single nucleotide polymorphisms (SNP) have been extensively investigated, as several of them have been shown to alter mRNA and/or protein expression levels. As P-gp determines the pharmacokinetics of several anticancer drugs, *MDR1* SNPs that affect P-gp expression and function have been of particular interest. A synonymous SNP in the *MDR1* gene, C3435T, which does not cause an amino acid substitution, was reported to be associated with low intestinal P-gp expression, low P-gp activity, and high digoxin absorption in individuals carrying this allele (14–16). Furthermore, our haplotype analysis has now further revealed that a *MDR1**2 haplotype with a linkage of C1236T *MDR1* (synonymous), G2677T *MDR1* (A893S P-gp), and C3435T *MDR1* is associated with a reduced renal excretion of irinotecan in Japanese cancer patients possibly due to a reduced P-gp function (17). However, the molecular mechanisms underlying the low renal excretion of irinotecan in this instance are still unclear.

Received 7/12/05; revised 12/25/05; accepted 1/25/06.

Grant support: Ministry of Education, Culture, Sports, Science and Technology and Ministry of Health, Labor and Welfare, Japan.

The costs of publication of this article were defrayed in part by the payment of page charges. This article must therefore be hereby marked advertisement in accordance with 18 U.S.C. Section 1734 solely to indicate this fact.

Requests for reprints: Yoshikazu Sugimoto, Department of Chemotherapy, Kyoritsu University of Pharmacy, 1-5-30 Shibakoen, Minato-ku, Tokyo 105-8512, Japan. Phone: 81-3-5400-2670; Fax: 81-3-5400-2669. E-mail: sugimoto-ys@kyoritsu-ph.ac.jp

doi:10.1158/1535-7163.MCT-05-0240

We have also reported previously the identification of a T3587G *MDR1* germ-line mutation in a Japanese patient, which confers a serine substitution for Ile^{1196} in P-gp (I1196S P-gp; ref. 17). We subsequently attempted to evaluate the possible functional alterations that may be caused by this substitution by analyzing the renal clearance of irinotecan in this individual who was heterozygous for the T3587G *MDR1*. There was an indication that the T3587G *MDR1* may be associated with high renal clearance of SN-38, but this observation was too preliminary to draw any firm conclusions as only one heterozygous patient was analyzed. This finding, however, prompted us to functionally characterize the Ser^{1196} substitution using *MDR1* cDNA-transfected cells and to further analyze additional Japanese subjects for the presence of other *MDR1* SNPs. We were subsequently able to identify a novel germ-line mutation in the *MDR1* gene, C3583T *MDR1*, which causes a substitution of tyrosine for His^{1195} in the P-gp (H1195Y P-gp). In our current study, we have established T3587G *MDR1* and C3583T *MDR1* cDNA transfectants and examined both expression levels and functional properties of I1196S P-gp and H1195Y P-gp. Our findings show that the T3587G *MDR1* cDNA encodes a nonfunctional P-gp and that the C3583T *MDR1* cDNA encodes a functional P-gp.

Materials and Methods

Sequence Analysis of the *MDR1* Gene

Peripheral blood nucleated cells were obtained from both healthy volunteers and cancer patients of Japanese nationality, after obtaining written informed consent, to undertake genetic analysis from each of these individuals. Exon 27 of the *MDR1* gene, which incorporates nucleotides 3,490 to 3,636 from the first ATG codon of the mRNA, was amplified by PCR from genomic DNA samples using the forward and reverse primers: 5′-CTTTACTTTCAGTTCTACTTTCA-3′ and 5′-GAGAATACAGCATTTTTAAGGA-3′, respectively. The resulting PCR products were directly sequenced using the primer 5′-CAGTTCTACTTTCATAACAACA-3′.

MDR1 Vectors

For the transfection of *MDR1* cDNA, we generated pCAL-MDR-IRES-ZEO bicistronic constructs, in which either wild-type (WT) or mutant *MDR1* cDNA insert was cloned upstream of the internal ribosome entry site (IRES) of the encephalomyocarditis virus. In the resulting transfectants, a single bicistronic mRNA species is transcribed under the control of the CAG promoter consisting of a cytomegalovirus immediate-early enhancer, a chicken β-actin transcription start site, and a rabbit β-globin intron (18). The upstream *MDR1* cDNA is translated in a cap-dependent manner, and the downstream *zeocin resistance gene* (*ZEO*) is translated under the control of the IRES.

For the retrovirus-mediated transfer of *MDR1* cDNAs, we constructed pHa-MDR-IRES-DHFR bicistronic retroviral vector plasmids, in which either WT or mutant *MDR1* cDNA insert was cloned upstream of the IRES.

Establishment of Mutant *MDR1* Transfectants

Murine fibroblast NIH3T3 cells were cultured in DMEM supplemented with 7% fetal bovine serum at 37°C in a humidified 5% CO_2 environment. For the establishment of WT or mutant *MDR1* transfectants, NIH3T3 cells were transfected with pCAL-MDR-IRES-ZEO containing either WT *MDR1*, C3583T *MDR1*, or T3587G *MDR1* cDNA. The cells were selected with 50 μg/mL zeocin and the resulting zeocin-resistant colonies were mixed. The zeocin-resistant mixed populations of the transfected cells were designated as 3T3/WT, 3T3/H1195Y, and 3T3/I1196S, respectively. Because 3T3/I1196S cells expressed only a small amount of P-gp, we isolated 30 T3587G *MDR1* cDNA transfectant clones by limiting dilution and tested for P-gp expression. A clone with the highest I1196S P-gp expression, designated as 3T3/I1196S clone 23, was used in the evaluation of ATP-binding activity of mutant P-gps.

The anticancer agent resistance levels in parental NIH3T3 cells and in the various *MDR1* transfectants were evaluated by cell growth inhibition assays after incubation of the cells for 5 days at 37°C in the absence or presence of various concentrations of vincristine or doxorubicin. Cell numbers were determined with a cell counter (Sysmex, Kobe, Japan).

Retrovirus-Mediated Mutant *MDR1* Gene Transfer

For retrovirus-mediated transfer of *MDR1* cDNAs, PA317 amphotropic retrovirus packaging cells were transfected with the pHa-MDR-IRES-DHFR plasmid containing either WT *MDR1*, C3583T *MDR1*, or T3587G *MDR1* cDNA insert using a calcium phosphate coprecipitation method. The transfectants were then selected by exposure to 120 ng/mL methotrexate and Ha-MDR-IRES-DHFR retrovirus-containing supernatants were harvested. NIH3T3 cells were then transduced with each of the Ha-MDR-IRES-DHFR retrovirus preparations following centrifugation at 2,800 rpm for 2 hours in the presence of polybrene (6 μg/mL) and cultured further in medium without retrovirus.

Fluorescence-Activated Cell Sorting Analysis of P-gp Expression

The expression levels of human P-gp on the cell surfaces of various *MDR1* transfectants were examined by fluorescence-activated cell sorting (FACS) analysis using a human-specific monoclonal antibody MRK16, which reacts with a cell surface epitope of P-gp. The cells were incubated with or without a biotinylated $F(ab')_2$ fragment of MRK16 (100 μg/mL) followed by washing and incubation with R-phycoerythrin-conjugated streptavidin (400 μg/mL; BD Biosciences, Franklin Lakes, NJ; ref. 19). Fluorescence staining levels were measured using FACSCalibur (BD Biosciences).

Western Blotting

Cell lysates of the *MDR1* transfectants were separated by SDS-PAGE and then electrotransferred onto a nitrocellulose membrane. The membrane was incubated with 1 μg/mL anti-P-gp monoclonal antibody C219 (Cencor, Malvern, PA; ref. 20) followed by washing and treatment with peroxidase-conjugated sheep anti-mouse secondary antibody (Amersham, Buckinghamshire, United Kingdom). The membrane-bound antibody was visualized with Enhanced Chemiluminescence Plus Detection kit (Amersham).

Genomic PCR and Reverse Transcription-PCR

Genomic DNA was extracted from each of the transfectants with a DNeasy Tissue kit (Qiagen, Valencia, CA) according to the manufacturer's instructions. *MDR1* cDNA (3,561 bp) was then amplified by PCR using the forward and reverse primers, 5′-CACGTGGTTGGAAGCTAACC-3′ and 5′-GAAGGCCAGAGCATAAGATGC-3′, respectively. As an internal control, the *glyceraldehyde-3-phosphate dehydrogenase* (*GAPDH*) gene (551-bp fragment) was amplified with the forward and reverse primers, 5′-ATCACCATCTTCCAGGAGCGA-3′ and 5′-GCTTCACCACCTTCTTGATGT-3′, respectively. The PCR conditions for *MDR1* amplification were as follows: 95°C for 5 minutes followed by 35 cycles of 95°C for 1 minute, 55°C for 1 minute, and 72°C for 3 minutes and a final extension at 72°C for 7 minutes. The *GAPDH* control amplification conditions were as follows: 95°C for 5 minutes followed by 20 cycles of 95°C for 30 seconds, 55°C for 30 seconds, and 72°C for 1 minute and a final extension at 72°C for 7 minutes.

The isolation of total RNA and subsequent reverse transcription-PCR was done using a RNeasy kit (Qiagen) and a RNA LA PCR kit (Takara, Ohtsu, Japan), each according to the manufacturer's instructions. First-strand *MDR1* cDNA was synthesized from 0.3 μg total RNA and a 702-bp *MDR1* cDNA fragment was amplified by PCR with the forward and reverse primers, 5′-GATATCAATGATACAGGGTT-3′ and 5′-TGTCCAATAGAATATTCCCC-3′, respectively. The PCR conditions were as follows: 95°C for 5 minutes followed by 18 to 24 cycles of 95°C for 30 seconds, 55°C for 30 seconds, and 72°C for 1 minute and a final extension at 72°C for 7 minutes. As an internal control, the amplification of *GAPDH* cDNA (551-bp fragment) was carried out as described above.

Vanadate-Induced Nucleotide Trapping in P-gp with 8-Azido-[α-32P]ATP

The ATP-binding activity of P-gp was examined by vanadate-induced nucleotide trapping analysis as described previously (21). Briefly, membrane fractions (5-20 μg) were prepared from *MDR1* transfectants and incubated with 10 μL buffer containing 10 μmol/L 8-azido-[α-^{32}P]ATP, 200 μmol/L orthovanadate, 3 mmol/L $MgCl_2$, 2 mmol/L ouabain, 0.1 mmol/L EGTA, and 40 mmol/L Tris-HCl (pH 7.5) in the absence or presence of 50 μmol/L verapamil for 10 minutes at 37°C. The reactions were stopped by the addition of 500 μL ice-cold TE buffer [40 mmol/L Tris-HCl (pH 7.5), 0.1 mmol/L EGTA]. The supernatants containing unbound ATP were removed from the membrane pellet after centrifugation (15,000 × *g*, 5 minutes, 4°C), and this procedure was repeated once more. The pellets were then resuspended in 8 μL TE buffer and irradiated for 5 minutes (at 254 nm, 8.2 mW/cm^2) on ice. The samples were then electrophoresed on a 7% SDS-polyacrylamide gel, electrotransferred to polyvinylidene difluoride membranes, and analyzed by autoradiography using a radioimaging analyzer (BAS2500, Fuji Photo Film Co., Tokyo, Japan). The polyvinylidene difluoride membranes were further analyzed by Western blotting with the anti-P-gp antibody C219. The P-gp expression levels were quantified using Scion Image software (Scion, Frederick, MD). The quantities of trapped 8-azido-[α-^{32}P]ATP in the WT and mutant P-gps, expressed as RI intensities in BAS2500, were normalized to the P-gp expression levels, and the relative photoaffinity labeling of each was then plotted. Two independent experiments were done, and the average of these analyses is shown.

Results

Frequency of the C3583T *MDR1* and T3587G *MDR1*

We identified previously a germ-line mutation of the *MDR1* gene, T3587G (17), in a Japanese cancer patient who was heterozygous for this allele and have now identified another germ-line mutation of the *MDR1* gene, C3583T, in a normal Japanese population. The C3583T *MDR1* and T3587G *MDR1* alleles encode H1195Y P-gp and I1196S P-gp, respectively, and both of the His^{1195} and Ile^{1196} residues are located in the Walker B region of the second ATP-binding site of P-gp (Fig. 1A). To examine the frequencies of occurrence for these mutations, we analyzed the genomic sequences of exon 27 of the *MDR1* gene, which incorporates the nucleotide region 3,490 to 3,636 of the mRNA. Of the 605 samples that we examined, two individuals were found to be heterozygous for the C3583T allele and an additional two subjects were found to be T3587G heterozygotes. Because of their low frequencies (<1%), C3583T *MDR1* and T3587G *MDR1* germ-line mutations would therefore be called naturally occurring base changes and not SNPs. We have not thus far identified any individuals who are homozygous for either of these mutations, nor have we observed individuals who are heterozygous for a combination of the C3583T and T3587G alleles.

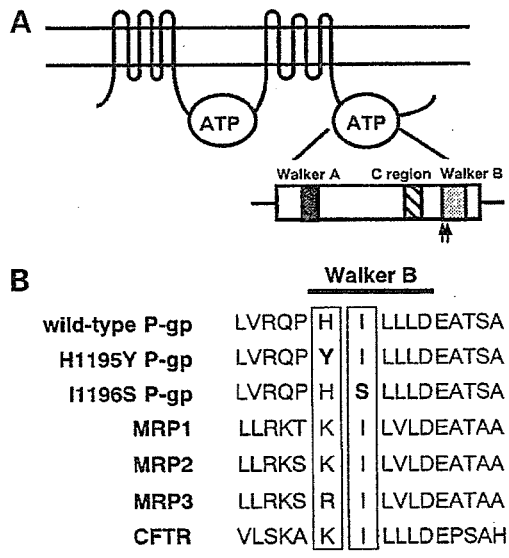

Figure 1. Map of specific mutations in P-gp. **A,** structure of P-gp. *Arrows,* location of the H1195Y and I1196S substitutions. **B,** alignment of various ATP-binding cassette transporter sequences close to the Walker B region of the second ATP-binding site. The His^{1195} and Ile^{1196} residues affected by the C3583T and T3587G mutations, together with the corresponding amino acids of other transporters, are boxed.

P-gp Expression Levels in the *MDR1* Transfectants

To investigate the molecular functions of the H1195Y mutant P-gp and I1196S mutant P-gp, we generated 3T3/WT, 3T3/H1195Y, and 3T3/I1196S cells, which were stably transfected with WT *MDR1*, C3583T *MDR1*, and T3587G *MDR1* cDNA, respectively. The P-gp expression levels on the cell surfaces of these transfectants were subsequently examined by FACS analysis using the MRK16 antibody, which recognizes a cell surface epitope of human P-gp. Both 3T3/WT and 3T3/H1195Y cells express P-gp on their cell surface, although these expression levels in 3T3/H1195Y cells (mean channel, 510) were slightly lower than in 3T3/WT cells (mean channel, 980; Fig. 2A). Surprisingly, the 3T3/I1196S cells did not express P-gp on their cell surface (Fig. 2A). We then examined the P-gp expression levels in the NIH3T3 cells and *MDR1* transfectants by Western blotting. In parental NIH3T3 cells, endogenous P-gp is expressed at very low levels (Fig. 2B). Moreover, both WT P-gp and H1195Y P-gp were detectable as a 145-kDa protein, whereas I1196S P-gp was observed as a 140-kDa protein (Fig. 2B). In addition, the expression levels of I1196S P-gp in 3T3/I1196S cells were at significantly lower levels than the other P-gp species.

As the expression levels of I1196S P-gp were very low in 3T3/I1196S cells, we examined the copy number of exogenous *MDR1* cDNA and the expression level of *MDR1* mRNA in these transfectants. A 3,561-bp human *MDR1* cDNA fragment, which is close to the full-length open reading frame, was amplified from genomic DNA isolates of the various *MDR1* cDNA transfectants. Each of the transfectants was found to have similar copy numbers of *MDR1* cDNA (Fig. 2C). We next did semiquantitative reverse transcription-PCR of *MDR1* mRNA in the transfectants. As shown in Fig. 2D, each of the *MDR1* transfectants also express similar levels of *MDR1* transcripts.

We then did retrovirus-mediated transfer of *MDR1* cDNAs to confirm the differences that we had observed in the expression levels of mutant P-gps. Amphotropic retrovirus was prepared from PA317 cells transfected with the pHa-MDR-IRES-DHFR vectors carrying either WT or mutant *MDR1* cDNA insert. NIH3T3 cells were then transduced with these *MDR1* retroviral preparations and the cells were cultured for 2 days and analyzed by FACS. As shown in Fig. 3, P-gp expression was observed in NIH3T3 cells transduced with both WT and H1195Y *MDR1* retroviruses but not in cells transduced with I1196S *MDR1* retrovirus. Transduction efficiencies were 70% and 60% for WT and H1195Y *MDR1* retroviruses, respectively. P-gp expression in cells transduced with H1195Y *MDR1* retrovirus was again found to be at a slightly lower levels than in cells transduced with WT *MDR1* retrovirus (Fig. 3B and C).

Drug Resistance in *MDR1* Transfectants

We next examined the drug resistance levels in our *MDR1* transfectants. 3T3/WT cells showed a 22-fold higher resistance to vincristine and 7-fold higher resistance to doxorubicin than parental NIH3T3 cells (Fig. 4). 3T3/H1195Y cells also showed higher levels of resistance to these drugs compared with the parental cells, but these were at slightly lower levels than 3T3/WT cells (Fig. 4). These findings correlated with the expression levels of P-gp

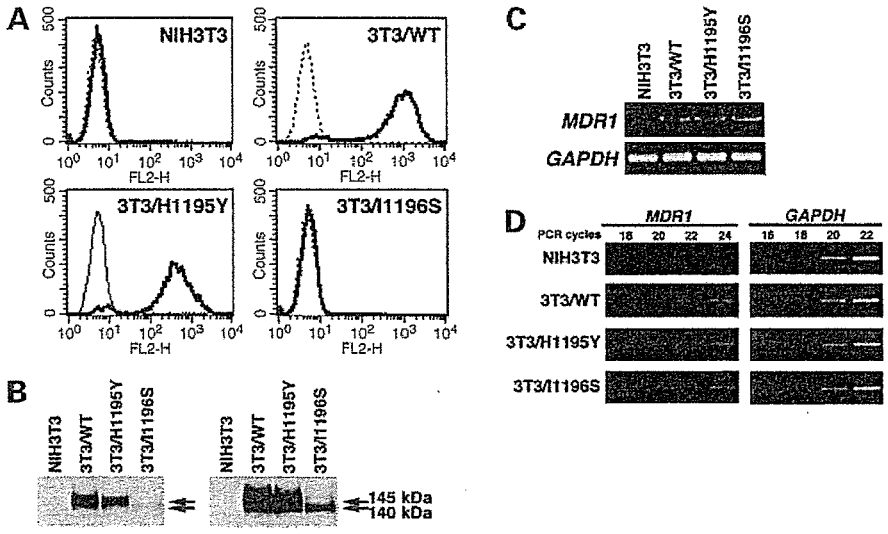

Figure 2. P-gp expression, *MDR1* cDNA integration, and *MDR1* mRNA expression in NIH3T3 transfectants. **A,** detection of cell surface expression of P-gp by FACS analysis. Parental NIH3T3 cells and the corresponding *MDR1* transfectants were harvested and then incubated with or without a biotinylated $F(ab')_2$ fragment of MRK16 followed by treatment with R-phycoerythrin-conjugated streptavidin. After washing, the fluorescence intensities were calculated using FACSCalibur. *Bold* and *dotted lines,* cells incubated with or without MRK16, respectively. **B,** Western blot analysis of P-gp in the *MDR1* transfectants. Protein extracts (20 μg) were subjected to Western immunoblotting analysis using the anti-P-gp monoclonal antibody C219 (1 μg/mL). *Left* and *right,* short (5 min) and long (15 min) exposures, respectively. **C,** genomic PCR analysis of exogenous *MDR1* cDNA in the *MDR1* transfectants. *MDR1* cDNA (3,561 bp) and *GAPDH* (551 bp) were amplified from genomic DNA preparations by PCR. *GAPDH* amplification was used as an internal control. **D,** reverse transcription-PCR analysis of *MDR1* transcripts in the NIH3T3 transfectants. *MDR1* (702 bp) and *GAPDH* (551 bp) transcripts were amplified by reverse transcription-PCR from 0.3 μg total RNA over the indicated number of cycles. *GAPDH* was again used as an internal control.

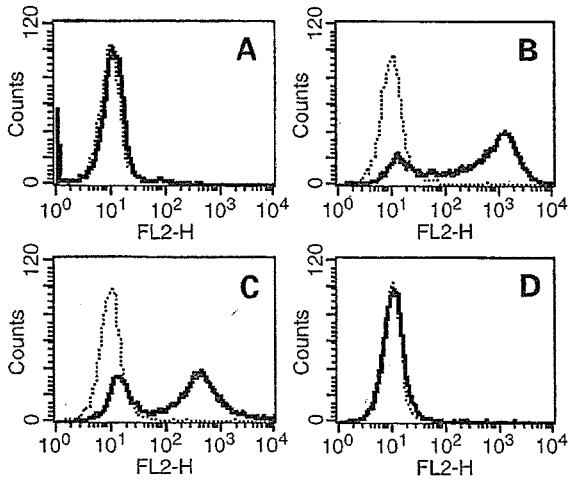

Figure 3. Cell surface expression of P-gp in retrovirally transduced cells. Cells were transduced with WT or mutant *MDR1* retroviruses, harvested, and incubated with or without a biotinylated $F(ab')_2$ fragment of MRK16 followed by treatment with R-phycoerythrin-conjugated streptavidin. After washing, the fluorescence intensities were calculated using FACSCalibur. *Bold* and *dotted lines*, cells incubated with or without MRK16, respectively. **A**, parental NIH3T3 cells. **B**, NIH3T3 cells transduced with WT *MDR1* retrovirus. **C**, NIH3T3 cells transduced with H1195Y *MDR1* retrovirus. **D**, NIH3T3 cells transduced with I1196S *MDR1* retrovirus.

in these cells and it is also significant that 3T3/I1196S cells showed no increased resistance to these chemotherapeutic agents when compared with the parental cells (Fig. 4), although I1196S P-gp was found to be expressed at low levels in 3T3/I1196S cells.

Loss of ATP-Binding Ability in I1196S P-gp

Because H1195Y P-gp and I1196S P-gp have amino acid substitutions in the second ATP-binding site of P-gp, we examined the ATP-binding activities of these variants. 3T3/I1196S clones were isolated and screened for higher P-gp expression, and clone 23 was found to contain the highest expression levels of I1196S P-gp. 3T3/I1196S clone 23 was thus used in these analyses (Fig. 5A). Because 3T3/I1196S clone 23 expressed ~25% of the WT P-gp levels, and 3T3/H1195Y cells expressed ~50% of the WT levels, we normalized these amounts in the relevant experiments (Fig. 5B and C). It was significant that the I1196S P-gp species showed no ATP-binding activity in either the absence or presence of 50 μmol/L verapamil (Fig. 5B and D). However, verapamil stimulated the nucleotide trapping of both WT P-gp and H1195Y P-gp, both of which showed similar levels of ATP-binding activity (Fig. 5C and D). These results suggest that I1196S P-gp lacks ATP-binding activity and therefore cannot function as an efflux pump.

Discussion

P-gp encoded by the *MDR1* gene is an important factor in the determination of the pharmacokinetics of its substrates, which include several anticancer drugs, as the coadministration of these agents and known P-gp inhibitors increases both the plasma concentration and the area under the concentration-time curve of these substrates (10, 11). C3435T *MDR1* was reported previously as a synonymous SNP that is associated with low intestinal P-gp expression, low P-gp activity, and high digoxin absorption (14). The association of a low level of P-gp activity was also observed with the *MDR1**2 haplotype containing C1236T *MDR1*, G2677T *MDR1*, and C3435T *MDR1* SNPs (17), but the details of the underlying mechanisms are still unknown. A *MDR1* SNP that causes a deficiency in P-gp function has not been reported previously.

In our previous and present studies, we have identified two nonsynonymous germ-line mutations, C3583T *MDR1* and T3587G *MDR1*. The C3583T *MDR1* substitutes a tyrosine for the His^{1195} residue of P-gp, whereas the T3587G *MDR1* results in a serine substitution for Ile^{1196}. Importantly, both of these residues are located in the Walker B region of the second ATP-binding site of P-gp (Fig. 1A). The Ile^{1196} residue in the P-gp is highly conserved among the members of ATP-binding cassette transporter superfamilies, but His^{1195} is not conserved among these proteins (refs. 22, 23; Fig. 1B). To examine the possible functional implications of these mutations, we established mutant *MDR1* cDNA transfectants and analyzed the biological consequences of the amino acid changes caused by these mutations.

Genetic variations have been known to affect mRNA expression and stability and also disrupt protein expression levels, turnover, and function. Because our study was designed to examine the possible effects of mutations in the coding region of the *MDR1* gene on protein expression levels, turnover, or function, we needed to establish WT or mutant *MDR1* transfectants that expressed similar amounts of *MDR1* mRNA. When standard two-promoter expression plasmid vectors are used for cDNA transfer, a high degree of variation in the expression of the transgene among transfectant clones may occur due to their different integration sites in the host genome and the possible effects of neighboring enhancers and/or silencers. We therefore

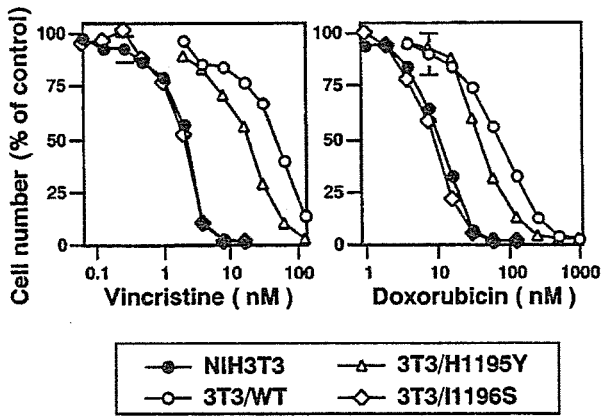

Figure 4. Drug resistance of the mutant *MDR1* transfectants. NIH3T3 (●), 3T3/WT (○), 3T3/H1195Y (△), and 3T3/I1196S (◇) cells were cultured for 5 d with various concentrations of vincristine or doxorubicin. Cell numbers were determined using a cell counter. *Points*, mean of triplicate experiments; *bars*, SD.

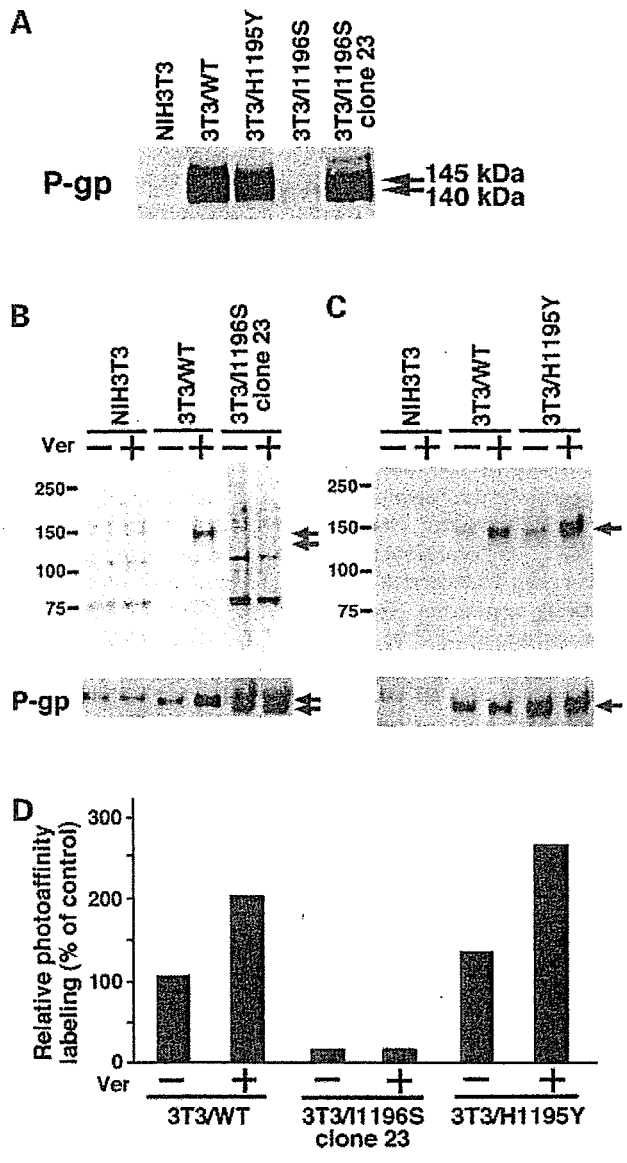

Figure 5. ATP-binding activities in the mutant *MDR1* transfectants. **A,** P-gp expression levels in the transfectants. Protein (20 μg) was loaded in each lane and subjected to Western blotting analysis using the anti-P-gp monoclonal antibody C219. **B,** ATP-binding activity of I1196S P-gp. Plasma membrane protein extracts of NIH3T3 (20 μg), 3T3/WT (5 μg), and 3T3/I1196S clone 23 (20 μg) cells were incubated with 10 μmol/L 8-azido-[α-^{32}P]ATP and 200 μmol/L vanadate in the absence (−) or presence (+) of 50 μmol/L verapamil for 10 min at 37°C. The proteins were then photoaffinity labeled by UV irradiation after the removal of unbound ligands and analyzed as described in Materials and Methods. *Top,* autoradiography using a radioimaging analyzer; *bottom,* Western blotting analysis of the same blot with the anti-P-gp antibody C219. *Arrows,* P-gps. **C,** ATP-binding activity of H1195Y P-gp. Plasma membrane protein extracts of NIH3T3 (20 μg), 3T3/WT (10 μg), and 3T3/H1195Y (20 μg) cells were analyzed as in **B.** *Top,* autoradiography using a radioimaging analyzer; *bottom,* Western blotting analysis of the same blot with the anti-P-gp antibody C219. *Arrows,* P-gps. **D,** relative ATP-binding activity of mutant P-gps. The trapped 8-azido-[α-^{32}P]ATP in the WT and mutant P-gps were quantified using BAS2500 imaging and normalized to the protein expression levels, and the relative photoaffinity labeling of each was then plotted. Two independent experiments were done, and the average of these analyses is shown.

used our previously reported flexible bicistronic vector system that uses an IRES to coexpress dominant drug-selectable markers, such as *dihydrofolate reductase* (*DHFR*) or *ZEO*, with the mutant *MDR1* gene (24, 25).

We reported previously the construction of bicistronic vectors in which the *MDR1* gene is coexpressed with herpes simplex virus-thymidine kinase (26–28), α-galactosidase A (28, 29), O^6-methylguanine DNA methyltransferase (30, 31), p47 of NADPH oxidase (32), and gp91 of NADPH oxidase (19, 33). We have further shown in this system that the drug treatments facilitated the enrichment or elimination of cells expressing the other nonselectable genes.

We next used this system to express mutant ATP-binding cassette transporters. We generated bicistronic pHa-BCRP-IRES-DHFR constructs to analyze the effects of *BCRP* coding SNPs on protein expression (34, 35). In the previous study, cells were transfected with pHa-BCRP-IRES-DHFR vectors containing either WT, G34A, C421A, or 944-949-deleted *BCRP* cDNA and then selected with methotrexate. In the resulting transfectants, a single mRNA is transcribed under control of a retrovirus long terminal repeat promoter, and two gene products are translated independently from a bicistronic mRNA. The upstream *BCRP* cDNA is translated cap-dependently, and the downstream *DHFR* cDNA is translated under a control of the IRES. Because only one mRNA species is transcribed, the cells expressing *DHFR* theoretically always coexpress the *BCRP* cDNA. We therefore combined all of the methotrexate-resistant colonies (>100) and used these mixed populations of methotrexate-resistant cells for further analysis. In this case, the expression of *BCRP* mRNA will reflect the mean levels for the transfectant clones and the mRNA levels within the mixed population will not be greatly affected by the expression levels of an individual clone. Indeed, we subsequently showed that four BCRP transfectants (mixed populations established after methotrexate selection) expressed similar levels of exogenous *BCRP* mRNA (34, 35). Additional FACS analysis then showed that almost all of the methotrexate-selected cells expressed BCRP on their cell surfaces. We then showed that BCRP expression from C421A *BCRP* cDNA is markedly lower than the WT.

In our present study, we constructed similar pCAL-MDR-IRES-ZEO bicistronic vectors that carry either WT or mutant *MDR1* cDNA insert. The transfectants were then selected with zeocin, and each of the resistant colonies (>100) were combined and used for further studies. As shown in Fig. 2A, most of the 3T3/WT and 3T3/H1195Y cells expressed cell surface P-gp. We also showed that the transfectants possess similar plasmid copy numbers (Fig. 2C) and similar levels of *MDR1* mRNA (Fig. 2D). To confirm our finding of a lower expression level of H1195Y P-gp, we did retrovirus-mediated gene transfer. Cells transduced with H1195Y *MDR1* retrovirus showed slightly lower P-gp expression levels than those transduced with WT *MDR1* retrovirus (Fig. 3). We therefore speculate that the difference in P-gp expression between 3T3/WT and 3T3/H1195Y cells is genuine and can be attributed to post-transcriptional events, such as protein maturation and/or stability.

Dubin-Johnson syndrome is an inherited disorder characterized by chronic conjugated hyperbilirubinemia due to the absence or dysfunction of the multidrug resistance-associated protein 2 (MRP2). Some Dubin-Johnson syndrome patients express mutant MRP2 proteins with amino acid substitutions or deletions (36–38). R768W MRP2, which has an amino acid substitution in signature C of the first ATP-binding site of the protein, is associated with relatively high serum bilirubin concentrations in affected patients (38) and this mutant protein is not properly glycosylated (36). Q1382R MRP2, a mutation that is located between the Walker A and the signature C regions of the second ATP-binding site, results in a lack of ATP hydrolysis activity (36). Moreover, the MRP2 mutant, which has a deletion in both its Arg^{1392} and Met^{1393} residues located between the Walker A and the signature C regions of the second ATP-binding site, is also a nonfunctional protein that shows impaired maturation and is sequestered in the endoplasmic reticulum (37). Hence, some MRP2 mutants that have mutations/deletions in the ATP-binding sites and lack ATP-hydrolyzing activity are underglycosylated, have not matured, and are unstable. We show in our current experiments that the I1196S P-gp also lacks ATP-binding activity and that its expression levels in 3T3/I1196S cells are markedly lower than in 3T3/WT cells. In addition, whereas the WT P-gp migrates as a 145-kDa protein, the I1196S P-gp migrates as a 140-kDa protein (Fig. 2B). The SDS-PAGE profile of I1196S P-gp is also very similar to the glycosylation-deficient P-gp that has the three amino acid substitutions, N91Q, N94Q, and N99Q (39). Taken together, these data suggest the possibility that I1196S P-gp does not undergo proper maturation, which results in low protein expression levels. Analyses of the biosynthesis and glycosylation status of I1196S P-gp are ongoing in our laboratory.

The conserved Asp^{1200} in the Walker B region of P-gp is required for the binding and hydrolysis of ATP (40, 41). Our present study also shows that substitution of serine for Ile^{1196} results in the loss of ATP-binding activity but that the substitution of tyrosine for His^{1195} does not affect P-gp function. It is not yet fully understood why mutant ATP-binding cassette transporters that lack ATP-binding activity are unstable, but defects in proper protein folding, particularly in ATP-binding sites, seem to be associated with protein degradation.

In our current study, we have also identified the T3587G and C3583T germ-line mutations in the *MDR1* gene in two individuals (0.3%) from a Japanese population of 605 individuals. In each case, however, these subjects were heterozygous for either the T3587G or C3583T allele. We contend, therefore, that there are two principal questions that arise from these findings: (*a*) the clinical significance of a homozygous T3587G *MDR1* genotype and (*b*) the clinical significance of a heterozygous T3587G *MDR1* genotype. Because the studies of *MDR1* double-knockout mice (*mdr1a/mdr1b−/−* mice) have shown that a *MDR1* deficiency causes large alterations in the pharmacokinetics of digoxin, vinblastine, and other drugs (12, 13), patients without P-gp function would also expected to show abnormal pharmacokinetics of P-gp substrate anticancer agents. Significantly, this may lead to potentially life-threatening side effects during cancer chemotherapy. Our present experiments have suggested the possible existence of a nonfunctional P-gp phenotype, but the extremely low allelic frequency of the T3587G *MDR1* mutation in our Japanese cohort makes it difficult to assess the relevance of a homozygous T3587G *MDR1* genotype in a clinical study. Hence, the existence of a subpopulation that has a high frequency of T3587G *MDR1* alleles would be necessary to detect homozygotes. It is likely that, in the absence of this, the prior genotype screening of homozygous T3587G *MDR1* patients undergoing cancer chemotherapy with P-gp substrate anticancer agents would be fruitless.

Another possible clinical study that could be undertaken would focus on T3587G *MDR1* heterozygous patients. We have identified heterozygous T3587G carriers in our Japanese population at a ratio of 1:300. In this regard, it is noteworthy that, in a previous report from our laboratory, a heterozygous T3587G *MDR1* patient treated with irinotecan showed the highest renal clearance of SN-38 among the group of irinotecan-treated patients in the study, although the renal clearances of irinotecan and SN-38 glucuronide in this individual were in the intermediate levels (17). However, it is not possible at this early stage to speculate on the effects of a heterozygous T3587G *MDR1* mutation from the results of only a single patient. To further clarify the consequences of a heterozygous T3587G allele, it will be necessary to further screen patients with T3587G *MDR1* mutation and examine whether they exhibit any aberrant kinetics or unusual toxicities as a result of treatments with *MDR1*-related anticancer agents. Such studies are currently ongoing in our laboratory and we wish to assess in the future whether the T3587G *MDR1* mutation would indeed be a candidate to be included in a putative SNP genotyping kit that would facilitate the screening of patients undergoing cancer therapy with P-gp substrates.

In a separate previous study from our laboratory, we identified the C376T *BCRP* SNP that encodes a Q126stop truncated BCRP (34, 35). The calculated frequency of homozygous C376T *BCRP* carriers was found to be 1.4 in 10,000, and we have not identified a homozygous carrier at this stage. Additionally, we have also reported that the C421A polymorphism in the *BCRP* gene, which substitutes lysine for the Gln^{141} residue of BCRP, is frequently observed in Japanese populations. Significantly, the Gln^{141} residue of BCRP lies between the Walker A and the signature C regions of its ATP-binding site. Moreover, Q141K BCRP-expressing cells show low levels of BCRP expression compared with WT BCRP-expressing cells (34, 35). This SNP may thus be important in the pharmacokinetics of irinotecan-related anticancer agents because cancer patients with the C421A allele show higher area under the concentration-time curve values after treatment with diflomotecan, an oral analogue of irinotecan, than patients harboring the WT allele (42). Hence, screening for SNPs that affect the expression of ATP-binding cassette and other transporters as well as drug-metabolizing enzymes are potentially very important for devising the appropriate treatments for cancer patients.

References

1. Riordan JR, Deuchars K, Kartner N, Alon N, Trent J, Ling V. Amplification of P-glycoprotein genes in multidrug-resistant mammalian cell lines. Nature 1985;316:817–9.

2. Chen CJ, Chin JE, Ueda K, et al. Internal duplication and homology with bacterial transport proteins in the *mdr1* (P-glycoprotein) gene from multidrug-resistant human cells. Cell 1986;47:381–9.

3. Shen DW, Fojo A, Chin JE, et al. Human multidrug-resistant cell lines: increased *mdr1* expression can precede gene amplification. Science 1986;232:643–5.

4. Gottesman MM, Hrycyna CA, Schoenlein PV, Germamm UA, Pastan I. Genetic analysis of the multidrug transporter. Annu Rev Genet 1995;29: 607–49.

5. Fojo AT, Ueda K, Slamon DJ, Poplack DG, Gottesman MM, Pastan I. Expression of a multidrug-resistance gene in human tumors and tissues. Proc Natl Acad Sci U S A 1987;84:265–9.

6. Cordon-Cardo C, O'Brien JP, Casals D, et al. Multidrug-resistance gene (P-glycoprotein) is expressed by endothelial cells at blood-brain barrier sites. Proc Natl Acad Sci U S A 1989;86:695–8.

7. Lown KS, Mayo RR, Leichtman AB, et al. Role of intestinal P-glycoprotein (mdr1) in interpatient variation in the oral bioavailability of cyclosporine. Clin Pharmacol Ther 1997;62:248–60.

8. van Asperen J, Schinkel AH, Beijnen JH, Nooijen WJ, Borst P, van Tellingen O. Altered pharmacokinetics of vinblastine in Mdr1a P-glycoprotein-deficient Mice. J Natl Cancer Inst 1996;17:994–9.

9. Hori R, Okamura N, Aiba T, Tanigawara Y. Role of P-glycoprotein in renal tubular secretion of digoxin in the isolated perfused rat kidney. J Pharmacol Exp Ther 1993;266:1620–5.

10. Merlin JL, Guerci A, Marchal S, et al. Comparative evaluation of S9788, verapamil, and cyclosporine A in K562 human leukemia cell lines and in P-glycoprotein-expressing samples from patients with hematologic malignancies. Blood 1994;84:262–9.

11. Mickisch GH, Kossig J, Keihauer G, Schlick E, Tschada RK, Alken PM. Effects of calcium antagonists in multidrug resistant primary human renal cell carcinomas. Cancer Res 1990;50:3670–4.

12. Schinkel AH, Wagenaar E, Mol CA, van Deemter L. P-glycoprotein in the blood-brain barrier of mice influences the brain penetration and pharmacological activity of many drugs. J Clin Invest 1996;97:2517–24.

13. Schinkel AH, Mayer U, Wagenaar E, et al. Normal viability and altered pharmacokinetics in mice lacking mdr1-type (drug-transporting) P-glycoproteins. Proc Natl Acad Sci U S A 1997;94:4028–33.

14. Hoffmeyer S, Burk O, von Richter O, et al. Functional polymorphism of the human multidrug resistance gene: multiple sequence variations and correlation of one allele with P-glycoprotein expression and activity *in vivo*. Proc Natl Acad Sci U S A 2000;97:3473–8.

15. Kurata Y, Ieiri I, Kimura M, et al. Role of human MDR1 gene polymorphism in bioavailability and interaction of digoxin, a substrate of P-glycoprotein. Clin Pharmacol Ther 2002;72:209–19.

16. Hitzl M, Drescher S, van der Kuip H, et al. The C3435T mutation in the human *MDR1* gene is associated with altered efflux of the P-glycoprotein substrate rhodamine 123 from $CD56^+$ natural killer cells. Pharmacogenetics 2001;11:293–8.

17. Sai K, Kaniwa N, Itoda M, et al. Haplotype analysis of *ABCB1/MDR1* blocks in a Japanese population reveals genotype-dependent renal clearance of irinotecan. Pharmacogenetics 2003;13:741–57.

18. Kiwaki K, Kanegae Y, Saito I, et al. Correction of ornithine transcarbamylase deficiency in adult spf(ash) mice and in OTC-deficient human hepatocytes with recombinant adenoviruses bearing the CAG promoter. Hum Gene Ther 1996;7:821–30.

19. Sugimoto Y, Tsukahara S, Sato S, et al. Drug-selected co-expression of P-glycoprotein and gp91 *in vivo* from an *MDR1*-bicistronic retrovirus vector Ha-MDR-IRES-gp91. J Gene Med 2003;5:366–76.

20. Kartner N, Evernden-Porelle D, Bradley G, Ling V. Detection of P-glycoprotein in multidrug-resistant cell lines by monoclonal antibodies. Nature 1985;316:820–3.

21. Takada Y, Yamada K, Taguchi Y, et al. Non-equivalent cooperation between the two nucleotide-binding folds of P-glycoprotein. Biochim Biophys Acta 1998;1373:131–6.

22. Payen LF, Gao M, Westlake CJ, Cole SPC, Deeley RG. Role of carboxylate residues adjacent to the conserved core Walker B motifs in the catalytic cycle of multidrug resistance protein 1 (ABCC1). J Biol Chem 2003;278:38537–47.

23. Ryu S, Kawage T, Nada S, Yamagichi A. Identification of basic residues involved in drug export function of human multidrug resistance-associated protein 2. J Biol Chem 2000;275:39617–24.

24. Sugimoto Y, Aksentijevich I, Gottesman MM, Pastan I. Efficient expression of drug-selectable genes in retroviral vectors under control of an internal ribosome entry site. Biotechnology 1994;12:694–8.

25. Zhang S, Sugimoto Y, Shoshani T, Pastan I, Gottesman MM. A pHaMDR-DHFR bicistronic expression system for mutation analysis of P-glycoprotein. Methods Enzymol 1998;292:474–80.

26. Sugimoto Y, Hrycyna C, Aksentijevich I, Pastan I, Gottesman MM. Co-expression of a multidrug resistahce gene (*MDR1*) and herpes simplex virus thymidine kinase gene as part of a bicistronic mRNA in a retrovirus vector allows selective killing of *MDR1*-transduced cells. Clin Cancer Res 1995;1:447–57.

27. Sugimoto Y, Sato S, Tsukahara S, et al. Coexpression of a multidrug resiatance gene (MDR1) and herpes simplex virus thymidine kinase gene in a bicistronic retroviral vector Ha-MDR-IRES-TK allows selective killing of *MDR1*-transduced human tumors transplanted in nude mice. Cancer Gene Ther 1997;4:51–8.

28. Sugimoto Y, Gottesman MM, Pastan I, Tsuruo T. Construction of *MDR1* vectors for gene therapy. Methods Enzymol 1998;292:523–37.

29. Sugimoto Y, Aksentijevich I, Murray GJ, Brady RO, Pastan I, Gottesman MM. Retroviral coexpression of a multidrug resistance gene (*MDR1*) and human α-galactosidase A for gene therapy of Fabry disease. Hum Gene Ther 1995;6:905–15.

30. Suzuki M, Sugimoto Y, Tsukahara S, Okochi E, Gottesman MM, Tsuruo T. Retroviral co-expression of two different types of drug-resistant genes to protect normal cells from combination chemotherapy. Clin Cancer Res 1997;3:947–54.

31. Suzuki M, Sugimoto Y, Tsuruo T. Efficient protection of cells from the genotoxicity of nitrosoureas by the retrovirus-mediated transfer of human O^6-methylguanine-DNA methyltransferase using bicistronic vectors with human multidrug resistance gene 1. Mutat Res 1998;410:133–41.

32. Iwata M, Nunoi H, Matsuda I, Kanegasaki S, Tsuruo T, Sugimoto Y. Drug-selected complete restoration of superoxide generation in Epstein-Barr virus-transformed B cells from p47phox-deficient chronic granulomatous disease patients using a bicistronic retrovirus vector encoding a human multidrug resistance gene (*MDR1*) and the *p47phox* gene. Hum Genet 1998;103:419–23.

33. Sokolic RA, Sekhsaria S, Sugimoto Y, et al. A bicistronic retrovirus vector containing a picornavirus internal ribosome entry site allows for correction of X-linked CGD by selection for *MDR1* expression. Blood 1996;87:42–50.

34. Imai Y, Nakane M, Kage K, et al. C421A polymorphism in the human breast cancer resistance protein gene is associated with low expression of Q141K protein and low-level drug resistance. Mol Cancer Ther 2002;1: 611–6.

35. Sugimoto Y, Tsukahara S, Ishikawa E, Mitsuhashi J. Breast cancer resistance protein: molecular target for anticancer drug resistance and pharmacokinetics/pharmacodynamics. Cancer Sci 2005;96:457–65.

36. Hashimoto K, Uchiumi T, Konno T, et al. Trafficking and functional defects by mutations of the ATP-binding domains in MRP2 in patients with Dubin-Johnson syndrome. Hepatology 2002;36:1236–45.

37. Keitel V, Kartenberk J, Nies AT, Spring H, Brom M, Keppler D. Impaired protein maturation of the conjugate export pump multidrug resistance protein 2 as a consequence of a deletion mutation in Dubin-Johnson syndrome. Hepatology 2000;32:1317–28.

38. Wada M, Toh S, Taniguchi K, et al. Mutations in the canalicular multispecific organic anion transporter (*cMOAT*) gene, a novel ABC transporter, in patients with hyperbilirubinemia II/Dubin-Johnson syndrome. Hum Mol Genet 1998;7:203–7.

39. Gribar JJ, Ramachandra M, Hrycyna CA, Dey S, Ambudkar SV. Functional characterization of glycosylation-deficient human P-glycoprotein using a vaccinia virus expression system. J Membr Biol 2000; 173:203–14.

40. Hrycyna CA, Ramachandra M, Germann UA, Cheng PW, Pastan I, Gottesman MM. Both ATP sites of human P-glycoprotein are essential but not symmetric. Biochemistry 1999;38:13887–99.

41. Urbatsch IL, Beaudet L, Carrier I, Gros P. Mutations in either nucleotide-binding site of P-glycoprotein (Mdr3) prevent vanadate trapping of nucleotide at both sites. Biochemistry 1998;37:4592–602.

42. Sparredoom A, Gelderblom H, Marsh S, et al. Diflomotecan pharmacokinetics in relation to ABCG2 421C>A genotype. Clin Pharmacol Ther 2004;76:38–44.

FEBS Letters 580 (2006) 4371–4376

Platelet derived growth factor regulates ABCA1 expression in vascular smooth muscle cells

Sachi Nagao[a], Koji Murao[a,*], Hitomi Imachi[a], Wen-Ming Cao[a], Xiao Yu[a], Junhua Li[a], Kensuke Matsumoto[a], Takamasa Nishiuchi[a], Rania A.M. Ahmed[a], Norman C.W. Wong[b], Kazumitsu Ueda[c], Toshihiko Ishida[a]

[a] *Division of Endocrinology and Metabolism, Department of Internal Medicine, Faculty of Medicine, Kagawa University, 1750-1 Ikenobe Miki-CHO, Kita-gun, Kagawa, Japan*

[b] *Departments of Medicine and Biochemistry & Molecular Biology, Faculty of Medicine, University of Calgary, Health Sciences Center, 3330 Hospital Drive NW, Calgary, Alta., Canada T2N 4N1*

[c] *Laboratory of Cellular Biochemistry, Division of Applied Life Sciences, Graduate School of Agriculture, Kyoto University, Kyoto 606-8502, Japan*

Received 10 May 2006; revised 20 June 2006; accepted 2 July 2006

Available online 10 July 2006

Edited by Laszlo Nagy

Abstract The ATP-binding cassette transporter A1 (ABCA1) regulates lipid efflux from peripheral cells to High-density lipoprotein. The platelet-derived growth factor (PDGF) is a potent mitogen that enables vascular smooth muscle cells to participate in atherosclerosis. In this report, we showed that PDGF suppressed endogenous expression of ABCA1 in cultured vascular smooth muscle cells. Exposure of CRL-208 cells to PDGF elicited a rapid phosphorylation of a kinase downstream from PI3-K, Akt. The constitutively active form of both p110, a subunit of PI3-K, and Akt inhibited activity of the ABCA1 promoter. In conclusion, PI3-K-Akt pathways participate in PDGF-suppression of ABCA1 expression.

Keywords: Platelet-derived growth factor; ATP-binding cassette transporter A1; Smooth muscle cell; Protein kinase B

1. Introduction

Atherosclerotic coronary artery disease (CAD) is a major public heath burden in developed countries. High-density lipoprotein (HDL) plays a critical role in cholesterol metabolism because they mediate a normal physiologic process, the so-called reverse cholesterol transport (RCT) [1,2]. In this process HDL particles shuttle cholesterol from extra-hepatic tissues to the liver for further metabolism and excretion [1]. The ATP-binding cassette transporter A1 (ABCA1), a 254-kDa membrane protein, is a pivotal regulator of lipid efflux from cells to apolipoproteins [3]. ABCA1 plays an important role in RCT because mutations of this gene found in patients with Tangier disease cause impaired efflux of lipids to apolipoprotein A–I [3].

Abnormal proliferation of vascular smooth muscle cells (VSMCs) is a critical component of atherosclerosis and arterial restenosis after angioplasty [4]. The mechanism is believed to be related to a response to injury in which growth factors such as a platelet derived growth factor (PDGF) are released, thus stimulating proliferation and migration of VSMCs to the site resulting in the formation of a neointima. PDGF bound to its receptor leads to the activation of several cell-signaling pathways associated with both VSMC proliferation and migration, such as those related to mitogen-activated protein kinase (MAPK), extracellular signal-regulated kinase (ERK) 1/2, phospholipase C-γ (PLC-γ), and phosphatidylinositol 3-kinase (PI3-k) [5]. Protein kinase B (Akt) activation is dependent on the upstream kinase PI3-K and influences cellular functions by activation of various downstream effectors [6].

In the present study, the results of our studies suggest that PDGF acts via the PI3-K/Akt signal transduction pathway to suppress ABCA1 gene transcription.

2. Materials and methods

2.1. Material

LY294002, PD98059, Bisindolylmaleimide I were purchased from Calbiochem (La Jolla, CA). Recombinant rat PDGF-BB was purchased from R&D, Co. Ltd (CA). Antibody: Anti-ABCA1 monoclonal antibody KM3110 was generated against the C-terminal 20 amino acids of ABCA1 in mice. Apolipoprotein A–I (apoA–I) and acetylated LDL (AcLDL) were purchased from Funakoshi (Osaka, Japan).

2.2. Plasmid preparation

An expression vector encoding a constitutively active Akt (Akt-CA) and a dominant-negative mutant of Akt (Akt-DN) was described previously [7]. An expression vector encoding a constitutively active p110 subunit was gift from J. Downward (Imperial Cancer research Foundation, London, UK). An expression vector encoding a PTEN (phosphatase and tensin homologue deleted on chromosome ten) was a gift from J.E. Dixon (Univ. of Michigan, Arbor, MI).

Cell culture: Primary cultured human vascular smooth muscle cell was purchased (Applied Cell Biology Research, Kirkland, WA). Rat vascular smooth muscle cell line, CRL-2018 (obtained from ATCC, Manassas, VA) was grown in DMEM (Life Technologies, Tokyo, Japan) supplemented with 10% FCS.

2.3. Western blot analysis

The proteins were resuspended under reducing conditions and a 15 μg was fractionated by size on 7.5% SDS–polyacrylamide gels [8]. The membranes were blocked overnight at room temperature with 0.1% Tween 20 in PBS (PBS-T) containing anti-ABCA1 antibody KM3110 (diluted 1:5000 from whole antiserum). These membranes

*Corresponding author. Fax: +81 878 91 2147.
E-mail address: mkoji@kms.ac.jp (K. Murao).

0014-5793/$32.00
doi:10.1016/j.febslet.2006.07.001

were washed with PBS-T, incubated for 1 h at room temperature in PBS-T containing horseradish peroxidase-linked anti-mouse IgG (diluted 1/3000), rinsed in PBS-T.

2.4. Transfection of CRL-2018 cells and luciferase reporter gene assay

The reporter construct contained the ABCA1 gene sequence spanning the region from −919 to +224 as determined from the published sequence [8]. The segment of interest was amplified using PCR and cloned into the luciferase reporter gene (pABCA1-LUC). Purified reporter plasmid was transfected into CRL-2018 cells using a conventional cationic liposome transfection method (Lipofectamine, Life Technologies, Gaithersburg, MD). All assays were corrected for β-galactosidase activity and total amount of protein in each reaction was identical as previously described [9].

2.5. Immunoblotting of Akt

Akt phosphorylated at Ser473 or Thr308 was detected using a phospho-specific Akt polyclonal antibody and total Akt was detected by using phosphorylation-independent antibodies (Upstate biotechnology, NY) as described previously [10]. The protein bands were visualized by chemiluminescence.

2.6. Cholesterol efflux assay

The cells were labeled with ^{3}H-cholesterol (5 μCi/ml) incorporated into acetylated LDL (AcLDL) (30 μg AcLDL/ml). Cells underwent an equilibration step in media plus 2 mg/ml bovine serum albumin (BSA) for 12 h prior to efflux. After the equilibration period, cells were incubated with apoA-I (30 μg/ml) in DMEM/BSA for 5 h. ^{3}H-cholesterol efflux was expressed as medium [^{3}H] cholesterol radioactivity as a percentage of total [^{3}H] cholesterol radioactivity [11].

2.7. Statistical analysis

Statistical comparisons were made possible through the use of one-way analysis of variance and Student's *t*-test, with $P < 0.05$ considered significant.

3. Results

3.1. PDGF decreases ABCA1 expression in CRL-2018 cells

To test whether PDGF affected ABCA1 expression, we used Western blot analysis to measure the levels of endogenous ABCA1 expression in both primary cultured human smooth muscle cell and cell line, CRL-2018. Exposure of the cells to PDGF for 24 h decreased the abundance of endogenous ABCA1 protein as compared with that in cells maintained in control media (Fig. 1A and B).

3.2. Effect of PDGF on ABCA1 promoter activity

Next we measured transcriptional activity of the ABCA1 promoter in the CRL-2018 cells. CRL-208 cells transfected with pABCA1-LUC were exposed to varying concentrations of PDGF (Fig. 2A). Consistent with the observed changes in the levels of ABCA1 protein and mRNA, PDGF inhibited activity of the promoter in a dose dependent fashion with near maximum inhibition using 10 ng/ml of PDGF. To test whether protein kinases were involved in the inhibitory actions of PDGF on ABCA1 promoter activity, we studied the effect of pharmacological inhibitors on ABCA1 promoter activity. Therefore, exposure of the pABCA1-LUC transfected CRL-2018 cells to PDGF (10 ng/ml) was tested in the presence of inhibitors such as PI3-K (10 μM LY294002), a mitogen-activated ERK (10 μM PD98059), or PKC (Bisindolylmaleimide I) to the CRL-2018 cells. Results (Fig. 2B) showed that the inhibitory effect of PDGF on ABCA1 promoter activity was not sensitive to inhibitors of ERK or PKC but it was sensitive to LY294002, an inhibitor of PI3-K.

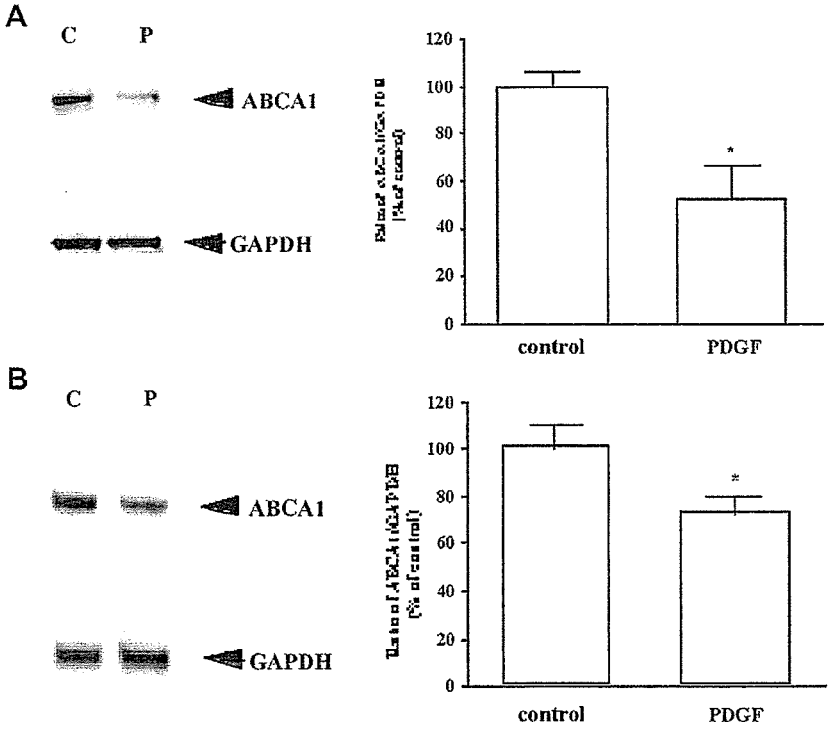

Fig. 1. Effect of PDGF on ABCA1 expression in CRL-2018 cells. (A,B) PDGF decreases ABCA1 protein expression. Human vascular smooth muscle cells (A) or CRL-2018 cells (B) were exposed to PDGF for 24 h and ABCA1 protein in total cell lysate was detected using Western blot analysis probed with an anti-ABCA1 antibody. (C) No-treatment or p: 10 ng/ml PDGF. A graph showing the mean ± S.E.M. of three experiments for each treatment group is shown on the right. The asterisk denotes a significant difference ($P < 0.01$).

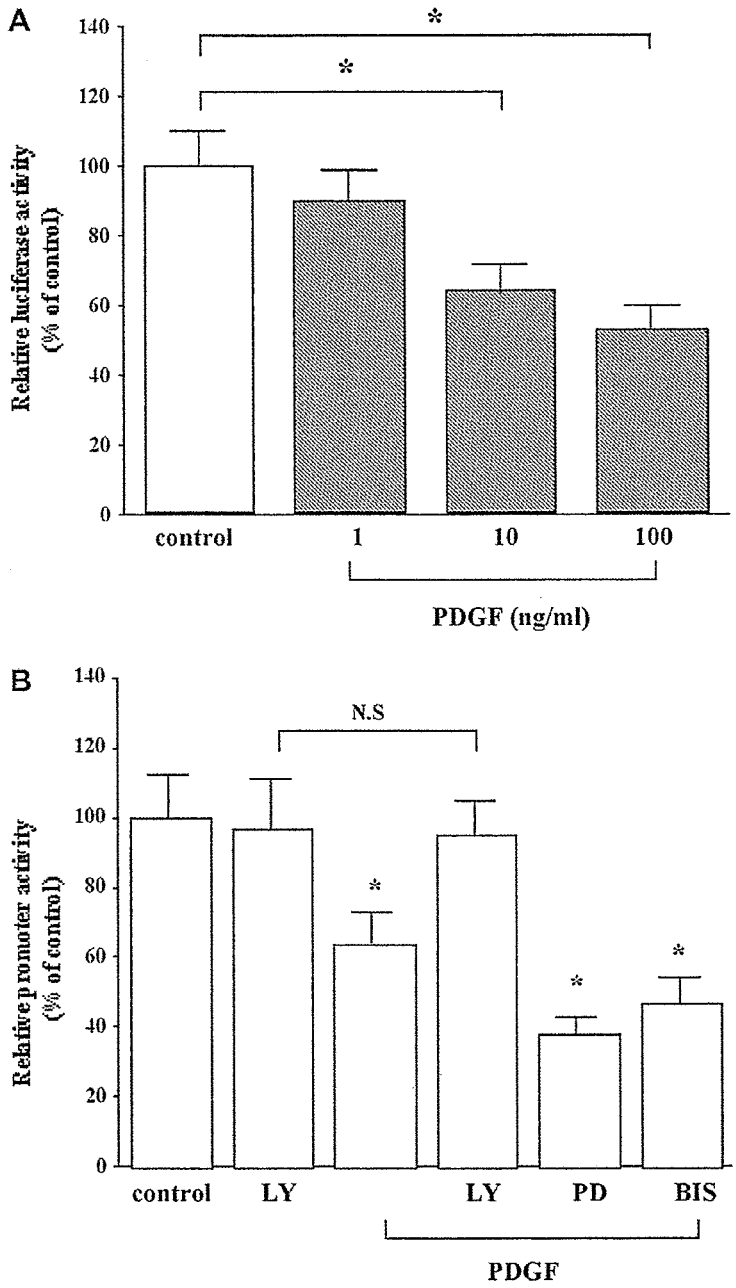

Fig. 2. Effect of PDGF on ABCA1 transcriptional activity and in CRL-2018 cells. (A) PDGF decreases ABCA1 gene transcription. CRL-2018 cells were transfected with pABCA1-LUC and treated with various concentration of PDGF for 24 h. Each data point shows the means ± S.E.M. of four separate transfections that were performed on separate days. The asterisk denotes a significant ($P < 0.01$). (B) A PI3-K inhibitor blocks the actions of PDGF. Effects of a PI3-K inhibitor LY294002 (LY), a MEK1 inhibitor PD98059 (PD), or a protein kinase C inhibitor Bisindolylmaleimide I (BIS) on PDGF (10 ng/ml)-inhibited ABCA1 transcriptional activity. Values represent the mean of triplicate determinations. The asterisk denotes a significant difference ($P < 0.01$).

3.3. Effect of PDGF on cholesterol efflux in CRL-2018 cells

To further demonstrate the inhibitory actions of PDGF, we took advantage of the fact that ABCA1 functions to facilitate cellular lipid efflux to HDL in the presence of ApoA–I [12]. This parameter was assessed by measuring cholesterol efflux from CRL-2018 cells to ApoA–I using ^{3}H-cholesterol delivered to the cells via acetylated-LDL uptake. We noted that pretreatment with PDGF (10 ng/ml) for 24 h proved to be most effective and therefore, all subsequent experiments were performed under these conditions. PDGF inhibited cholesterol efflux to 75% of control untreated cells (Fig. 3). As predicted from the preceding studies, LY294002 blocked PDGF-suppression of the cholesterol efflux but the PI3-K inhibitor had no stimulatory effect on basal efflux in the absence of PDGF.

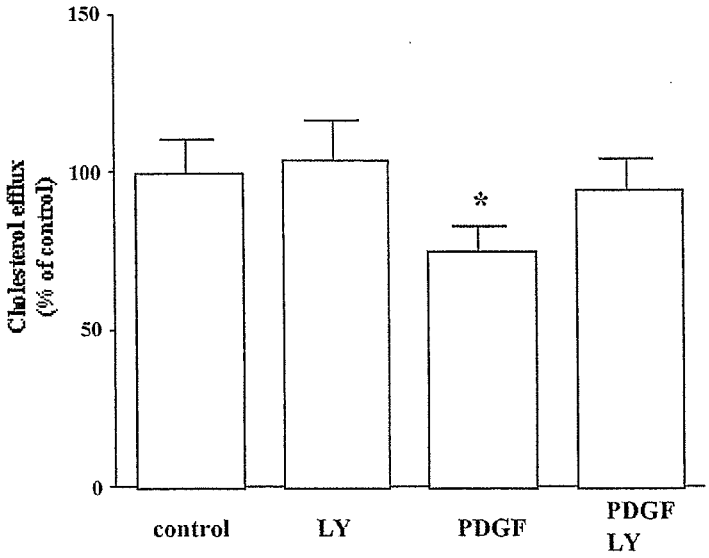

Fig. 3. PDGF inhibits cholesterol efflux in CRL-2018 cells. CRL-2018 cells were treated with PDGF (10 ng/ml), LY294002 (LY), or both PDGF and the inhibitor. The cells were incubated with apoA–I (50 μg/ml) in DMEM/BSA for 5 h. ApoA–I specific [^{3}H] cholesterol efflux was calculated and apoA–I-specific efflux in the absence of any treatment was normalized to 100%. Each individual experiment was performed in quadruplicate and the values show the mean ± S.E.M. The asterisk denotes a significant difference ($P < 0.01$). Lane 1; control, lane2; LY294002 (LY), lane 3; PDGF, lane 4; PDGF and LY294002 (LY).

3.4. Time course of Akt phosphorylation by PDGF

The preceding studies showed that PI3-kinase likely participated in the inhibitory effects of PDGF on ABCA1 expression. Since Akt is a potential target of the PI3-K, we wondered whether the use of PDGF could also activate Akt. To answer this question, we examined the kinetics of Akt activation by measuring phosphorylation of the residues Thr308 and Ser473. These sites are modified as a prerequisite for catalytic activity of Akt. The results (Fig. 4) showed that Akt phosphorylation was evident within 15 min following exposure of the CRL-2018 cells to PDGF and this activity reached a peak at 60 min.

3.5. Akt regulates ABCA1 promoter activity

Since Akt phosphorylation may participate in PDGF inhibition of ABCA1 expression, we asked whether Akt affected ABCA1 promoter activity. If so, then the actions of constitutively active Akt, p110 (a subunit of PI3-K), and PTEN (a natural inhibitor of PI3-K pathway) should affect activity of the promoter. As predicted, the results (Fig. 5A) showed that constitutively active Akt and p110 suppressed ABCA1 promoter activity in CRL-2018 cells. In contrast, the co-transfection of PTEN expression vector activated pABCA1-LUC activity.

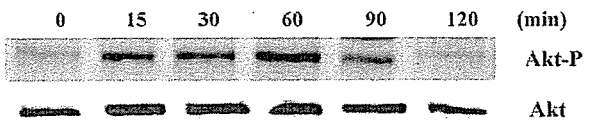

Fig. 4. PDGF stimulates the phosphorylation of Akt. CRL-2018 cells were exposed to 10 ng/ml PDGF for 0, 15, 30, 60, 90 and 120 min. Abundance of phosphorylated Akt was detected by Western blot analysis using a phospho-specific Akt antibody (Akt-P, upper portion). To show equal loading of protein in the each lane, the same blot was probed a second time with an Akt-specific antibody.

To further confirm the role of Akt, we tested the effects of a dominant negative mutant of Akt (Akt-DN) on ABCA1 promoter activity (Fig. 5B). Consistent with the above studies; PDGF inhibited the activity of the ABCA1 promoter and the expression of Akt-DN inhibited the actions of PDGF on ABCA1 promoter activity.

4. Discussion

In this report, we have summarized the results of studies showing that PDGF affected ABCA1 gene expression. To connect the actions of Akt with ABCA1 expression, we assessed the effects of both a constitutively active and a dominant negative form of Akt on ABCA1 promoter activity (Fig. 5). In agreement with our hypothesis, constitutively activated Akt mimiced the inhibitory action of PDGF on ABCA1 promoter activity and the dominant negative mutant blocked this effect. Further studies of the role of Akt in PDGF-mediated ABCA1 inhibition will be necessary to define the pathway by which PDGF affects the gene.

Since Akt/PKB is one of the downstream components of intracellular signaling triggered by PDGF, it is not surprising that Akt/PKB was phosphorylated following treatment of CRL-2018 cells with PDGF. Akt/PKB phosphorylation is negatively regulated by PTEN/MMAC1/TEP1 a tumor suppressor gene product. This protein is a phosphatase that dephosphorylates the 3′ position to reverse the reactions catalyzed by PI3-K [13]. Results in Fig. 5A showed that overexpression of PTEN increased ABCA1 promoter activity.

Many studies indicate that phenotypic modulation of SMC within atherosclerotic lesions is very complex and likely to involve many factors including growth factors and cytokines, inflammatory cell mediators, lipids, lipid peroxidation products, and reactive oxygen species [14,15]. Platelet-derived

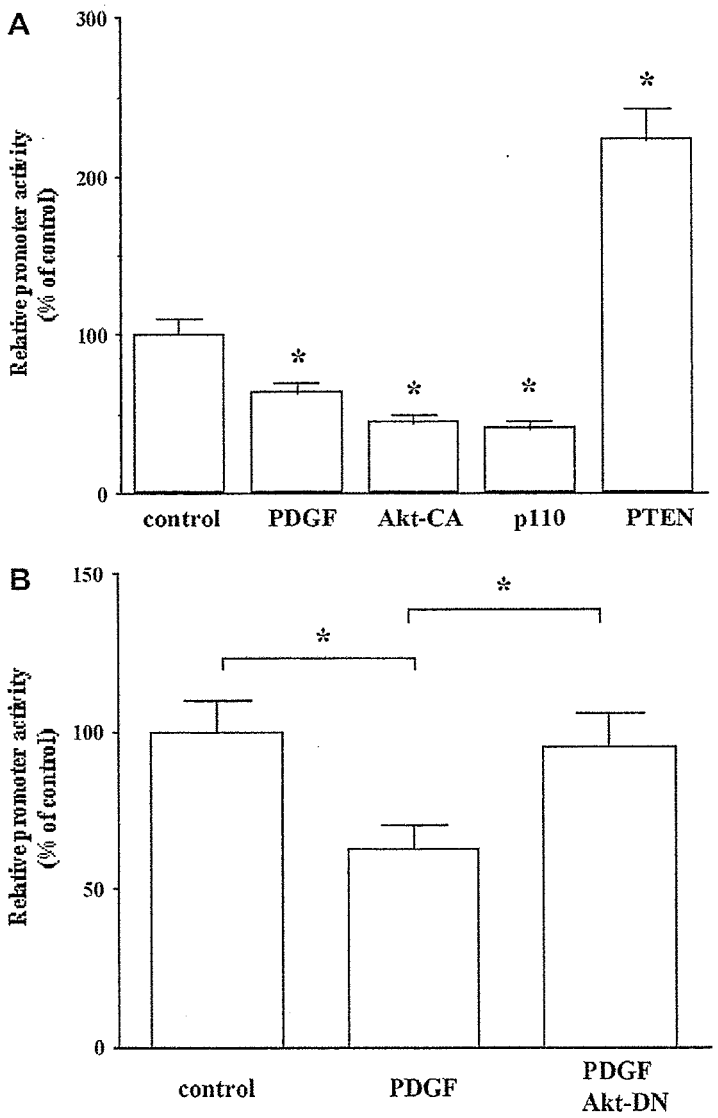

Fig. 5. Role of PI3-K/Akt signal transduction pathway on ABCA1 promoter activity by PDGF. (A) Effects of PI3-K components on ABCA1 promoter activity. CRL-2018 cells were transfected with pABCA1-LUC and empty vector (Cont), empty vector plus PDGF-treatment (PDGF), Akt-CA expression vector (Akt-CA), p110 expression vector (p110), and PTEN expression vector (PTEN). Each data point shows the means ± S.E.M. of four separate transfections that were performed on separate days. The asterisk denotes a significant difference ($P < 0.01$). (B) Dominant negative Akt blocks PDGF inhibition of ABCA1 transcription. CRL-2018 cells were transfected with pABCA1-LUC and empty vector or Akt-DN and then treated with PDGF. Each data point shows the means ± S.E.M. of four separate transfections that were performed on separate days. The asterisk denotes a significant difference ($P < 0.01$).

growth factor (PDGF) is a potent mitogen and chemoattractant that functions as an important mediator in the pathogenesis of vascular disease [16]. Our studies showed that inhibition of PI3-K completely blocked the effect of PDGF-suppressed ABCA1 promoter activity in VSMCs, whereas MEK1 and PKC inhibitors had no effect on this action, the PI3-K inhibitor LY294002 prevented the suppressive effects of PDGF. Although those pharmacological probes are relatively selective, we also verified the results by using the constitutively active form of p110, the subunit of PI3-K and PTEN, the natural inhibitor of PI3-K pathway. The concordance between the data using pharmacological probes and the constitutively active constructs provides evidence that ABCA1 gene expression is regulated by a PI3-K-dependent pathway. FoxO transcription factors have been implicated in regulating diverse cellular functions including differentiation, metabolism, proliferation, and survival. Furthermore, it is well acknowledged that Akt mediates many of the effect of growth factors downstream of PI3-K, and several FoxO proteins are now established substrates of Akt in this pathway [17]. We identified a putative FoxO response sequence on ABCA1 promoter by searching the BLASTN program in a genomic database. Further studies will be needed to determine the detailed mechanisms involved in the regulation of the ABCA1 gene.

In summary, the results in this report show that PDGF inhibits the expression of the endogenous ABCA1 in rat

vascular smooth muscle cell line, CRL-2018. This inhibitory effect of PDGF on ABCA1 promoter is mediated by PI3-K/Akt signal transduction pathway. These findings raise the possibility that PDGF may affect RTC by controlling ABCA1 expression.

References

[1] Fielding, C.J. and Fielding, P.E. (1995) Molecular physiology of reverse cholesterol transport. J. Lipid. Res. 36, 211–228.

[2] Tall, A.R. (1990) Plasma high density lipoproteins. Metabolism and relationship to atherogenesis. J. Clin. Invest. 86, 379–384.

[3] Tall, A.R. and Wang, N. (2000) Tangier disease as a test of the reverse cholesterol transport hypothesis. J. Clin. Invest. 106, 1205–1207.

[4] Newby, A.C. and Zaltsman, A.B. (2000) Molecular mechanisms in intimal hyperplasia. J. Pathol. 190, 300–309.

[5] Homma, Y., Sakamoto, H., Tsunoda, M., Aoki, M., Takenawa, T. and Ooyama, T. (1993) Evidence for involvement of phospholipase C-gamma 2 in signal transduction of platelet-derived growth factor in vascular smooth-muscle cells. Biochem. J. 290, 649–653.

[6] Shiojima, I. and Walsh, K. (2002) Role of Akt signaling in vascular homeostasis and angiogenesis. Circ. Res. 90, 1243–1250.

[7] Cao, W.M., Murao, K., Imachi, H., Sato, M., Nakano, T., Kodama, T., Sasaguri, Y., Wong, N.C., Takahara, J. and Ishida, T. (2001) Phosphatidylinositol 3-OH kinase-Akt/protein kinase B pathway mediates Gas6 induction of scavenger receptor a in immortalized human vascular smooth muscle cell line. Arterioscler. Thromb. Vasc. Biol. 21, 1592–1597.

[8] Langmann, T., Porsch-Ozcurumez, M., Heimerl, S., Probst, M., Moehle, C., Taher, M., Borsukova, H., Kielar, D., Kaminski, W.E., Dittrich-Wengenroth, E. and Schmitz, G. (2002) Identification of sterol-independent regulatory elements in the human ATP-binding cassette transporter A1 promoter: role of Sp1/3, E-box binding factors, and an oncostatin M-responsive element. J. Biol. Chem. 277, 14443–14450.

[9] Murao, K., Wada, Y., Nakamura, T., Taylor, A.H., Mooradian, A.D. and Wong, N.C. (1998) Effects of glucose and insulin on rat apolipoprotein A–I gene expression. J. Biol. Chem. 273, 18959–18965.

[10] Cao, W.M., Murao, K., Imachi, H., Yu, X., Dobashi, H., Yoshida, K., Muraoka, K., Kotsuna, N., Nagao, S., Wong, N.C. and Ishida, T. (2004) Insulin-like growth factor-I regulation of hepatic scavenger receptor class BI. Endocrinology 145, 5540–5547.

[11] Kiss, R.S., McManus, D.C., Franklin, V., Tan, W.L., McKenzie, A., Chimini, G. and Marcel, Y.L. (2003) The lipidation by hepatocytes of human apolipoprotein A–I occurs by both ABCA1-dependent and -independent pathways. J. Biol. Chem. 278, 10119–10127.

[12] Singaraja, R.R., Brunham, L.R., Visscher, H., Kastelein, J.J. and Hayden, M.R. (2003) Efflux and atherosclerosis: the clinical and biochemical impact of variations in the ABCA1 gene. Arterioscler. Thromb. Vasc. Biol. 23, 1322–1332.

[13] Maehama, T. and Dixon, J.E. (1998) The tumor suppressor, PTEN/MMAC1, dephosphorylates the lipid second messenger, phosphatidylinositol 3,4,5-trisphosphate. J. Biol. Chem. 273, 13375–13378.

[14] Lusis, A.J. (2000) Atherosclerosis. Nature 407, 233–241.

[15] Ross, R. (1999) Atherosclerosis – an inflammatory disease. N. Engl. J. Med. 340, 115–126.

[16] Seewald, S., Sachinidis, A., Seul, C., Kettenhofen, R., Ko, Y. and Vetter, H. (1997) The role of platelet-derived growth factor-BB-induced increase in cytosolic free Ca2+ in activation of mitogen-activated protein kinase and DNA synthesis in vascular smooth muscle cells. J. Hypertens. 15, 1671–1675.

[17] Accili, D. and Arden, K.C. (2004) FoxOs at the crossroads of cellular metabolism, differentiation, and transformation. Cell 117, 421–426.

THE JOURNAL OF BIOLOGICAL CHEMISTRY VOL. 281, NO. 16, pp. 10760–10768, April 21, 2006

Purification and ATPase Activity of Human ABCA1*[S]

Received for publication, December 27, 2005, and in revised form, February 15, 2006 Published, JBC Papers in Press, February 24, 2006, DOI 10.1074/jbc.M513783200

Kei Takahashi, Yasuhisa Kimura, Noriyuki Kioka, Michinori Matsuo, and Kazumitsu Ueda[1]

From the Laboratory of Cellular Biochemistry, Division of Applied Life Sciences, Graduate School of Agriculture, Kyoto University, Kyoto 606-8502, Japan

ATP-binding cassette protein A1 (ABCA1) plays a major role in cholesterol homeostasis and high density lipoprotein metabolism. Apolipoprotein A-I binds to ABCA1 and cellular cholesterol and phospholipids, mainly phosphatidylcholine, are loaded onto apoA-I to form pre-β high density lipoprotein (HDL). It is proposed that ABCA1 translocates phospholipids and cholesterol directly or indirectly to form pre-β HDL. To explore the mechanism of ABCA1-mediated pre-β HDL formation, we expressed human ABCA1 in insect Sf9 cells and purified it. Trypsin limited-digestion of purified ABCA1 in the detergent-soluble form suggested that it retained conformation similar to ABCA1 expressed in the membranes of human fibroblast WI-38 cells. Purified ABCA1 showed robust ATPase activity when reconstituted in liposomes made of synthetic phosphatidylcholine. ABCA1 showed lower ATPase activity when reconstituted in liposomes containing phosphatidylserine, phosphatidylethanolamine, or phosphatidylglycerol and also showed weak specificity in acyl chain species. ATPase activity was reduced by the addition of cholesterol and decreased by 25% in the presence of 20% cholesterol. β-Sitosterol and campesterol showed similar inhibitory effects but stigmasterol did not, suggesting structure-specific interaction between ABCA1 and sterols. Glibenclamide suppressed ABCA1 ATPase, suggesting that it inhibits apoA-I-dependent cellular cholesterol efflux by suppressing ABCA1 ATPase activity. These results suggest that the ATPase activity of ABCA1 is stimulated preferentially by phospholipids with choline head groups, phosphatidylcholine and sphingomyelin. This study with purified human ABCA1 provides the first biochemical basis of the mechanism for HDL formation mediated by ABCA1.

ATP-binding cassette protein A1 (ABCA1)[2] plays a major role in cholesterol homeostasis and high density lipoprotein (HDL) metabolism. It has been reported that apolipoprotein A-I (apoA-I) binds to ABCA1 and cellular free cholesterol (FC) and phospholipids (PL) are loaded onto apoA-I to form pre-β HDL. It is clear that ABCA1 is involved in phosphatidylcholine (PC)-rich HDL generation in plasma, because plasma PL concentration of *Abca1*−/− mice was decreased by more than 75%, mostly due to a reduction of PC in HDL (1); however, the molecular mechanism behind ABCA1-mediated pre-βHDL formation is still poorly understood.

Several models have been proposed for the mechanism of ABCA1-mediated pre-β HDL formation: (*a*) a two-step process model proposed by Fielding *et al.* (2) and Wang *et al.* (3): ABCA1 first mediates PL efflux to apoA-I, and this apolipoprotein-PL complex accepts FC in an ABCA1-independent manner. This model is based on two types of experiments: (i) vanadate, glibenclamide, and cyclodextrin show differential inhibitory effects upon PL and FC efflux to apoA-I, and (ii) medium containing apoA-I conditioned on smooth muscle cells leads to FC efflux from vascular endothelial cells that do not express ABCA1. (*b*) A concurrent process model: FC and PL efflux by ABCA1 to apoA-I are tightly coupled to each other (4). (*c*) PS flipping model: ABCA1 mediates the translocation of PS to the outer leaflet, and extracellular exposure of PS promotes apoA-I binding to the cell surface and subsequent translocation of PC and cholesterol to apoA-I (5).

ABC proteins involved in xenobiotic efflux, such as MDR1 and MRP1, harness the energy liberated from ATP to drive the conformation changes that move xenobiotics across the membrane, and mutations in the ATP binding domain abolish the transport activity of these proteins (6, 7). Like these xenobiotic transporters, ABCA1 K939M mutant, in which lysine, indispensable for the hydrolysis of ATP by various ABC proteins (8–11), was substituted by methionine, was impaired in apoA-I-dependent PL and cholesterol efflux (3, 5). As the translocation (flip-flop) of PLs rarely spontaneously occurs in lipid bilayers, and this process is highly energy-dependent, ABCA1 is suggested to flip-flop PLs depending on ATP hydrolysis. However, because the ABCA1 K939M mutant is defective in its interaction with apoA-I (3, 5), it is also possible that ATP binding and/or ATP hydrolysis cause conformational changes of ABCA1, which are required for the interaction with apoA-I, and ABCA1 functions as a regulator in HDL formation (12) as SUR does in the ATP-sensitive potassium channel complex (13).

Human ABCA7, which has the highest homology (66.1%) to ABCA1, mediates the apoA-I-dependent efflux of phospholipids and cholesterol as ABCA1 (14); however, human ABCA7 mediates cholesterol release with much less efficiency than ABCA1 (15), and it has been reported that phospholipids but not cholesterol are loaded onto apoA-I by mouse ABCA7 (16). These results may not be explained by the two-step process model and suggest that ABCA1 and ABCA7 have different substrate specificities for transport and that cholesterol is one of the transport substrates for ABCA1.

To explore the mechanism of ABCA1-mediated pre-β HDL formation, we purified human ABCA1 as a detergent-soluble form and examined ATPase activity. Purified ABCA1 showed robust ATPase activity when reconstituted in liposomes made of synthetic PC, and the ATPase

* This work was supported by Grant-in-aid for Scientific Research and Creative Scientific Research 15GS0301 from the Ministry of Education, Culture, Sports, Science, and Technology, Japan, and grants from the Bio-oriented Technology Research Advancement Institution (BRAIN), and the Pharmaceutical and Medical Devices Agency. The costs of publication of this article were defrayed in part by the payment of page charges. This article must therefore be hereby marked "*advertisement*" in accordance with 18 U.S.C. Section 1734 solely to indicate this fact.

[S] The on-line version of this article (available at http://www.jbc.org) contains supplemental Figs. 1–4.

[1] To whom correspondence should be addressed. Tel.: 81-75-753-6124; Fax: 81-75-753-6104; E-mail: uedak@kais.kyoto-u.ac.jp.

[2] The abbreviations used are: ABCA1, ATP-binding cassette protein A1; ABCA1 MM, ABCA1 K939M-K1952M; MDR, multidrug resistance; MRP, multidrug resistance-related protein; NBF, nucleotide-binding fold; apo, apolipoprotein; HDL, high density lipoprotein; FC, free cholesterol; PL, phospholipid; PC, phosphatidylcholine; PS, phosphatidylserine; PE, phosphatidylethanolamine; SM, sphingomyelin; PG, phosphatidylglycerol; POPC, 1-palmitoyl-2-oleoylphosphatidylcholine; DPPC, 1,2-dipalmitoylphosphatidylcholine; POPS, 1-palmitoyl-2-oleoylphosphatidylserine; DPPE, 1,2-dipalmitoylphosphatidylethanolamine; DPPG, 1,2-dipalmitoylphosphatidylglycerol; Sf9, *Spodoptera frugiperda* 9; HEK, human embryo kidney; NGF, *N*-glycosidase F; DDM, *n*-dodecyl-β-D-maltoside; NTA, nitrilotriacetic acid.

activity was inhibited by glibenclamide but not by vanadate. ABCA1 ATPase was reduced by the addition of cholesterol.

EXPERIMENTAL PROCEDURES

Materials—Bovine serum albumin, leupeptin, aprotinin, trypsin, glibenclamide, stigmasterol, campesterol, and Na_2ATP were purchased from Sigma. Baculovirus transfer vector (pVL1392) and baculovirus (Baculogold™) were obtained from Invitrogen. Anti-penta-His antibody was obtained from Qiagen. L-α-Lecitin (20%) from soybean and sphingomyelin from egg yolk were obtained from Sigma. Synthesized phospholipids, PC, phosphatidylserine (PS), phosphatidylethanolamine (PE), phosphatidylglycerol (PG), and cholesterol were purchased from Avanti polar lipids. β-Sitosterol and brassicasterol were purchased from Tama Biochemical Co., Ltd. Other chemicals were purchased from Wako Pure Chemical Industries Ltd. KM3073 monoclonal antibody was generated against the first extracellular domain (35–635 amino acid) of human ABCA1 in rats as described previously (17). Anti-ABCA1 NBF2 rabbit polyclonal antibody, which specifically interacts with the second nucleotide binding fold (NBF2) (data not shown), was generated against the purified NBF2 of human ABCA1 (1908–2159 amino acids). Anti-ABCA1 C terminus rabbit antibody was a kindly gift from Dr. Shinji Yokoyama, Nagoya City University Graduate School of Medical Sciences.

Construction of Transfer Vector—The 3′ end of human ABCA1 cDNA (18) was modified by elimination of the natural termination codon and insertion of a supplementary sequence containing a thrombin cleavage site, a biotinylation tag, and 10 consecutive histidine residues before the termination codon (5′-CTAGACTGGTTCCGCGTGGTTCCGGCTTGAATGATATATTCGAGGCCCAGAAGATAGAGTGGCATGAGGGAACTAGACTGGTTCCGCGTGGTTCCCACCATCACCATCACCATCACCATCACCATTGAG-3′). The modified ABCA1 cDNA (designated ABCA1-TATH) was inserted into the transfer vector pVL1392. To construct the NBF1 Walker A lysine mutant, ABCA1 K939M, DNA fragments containing a K939M missense mutation were generated by a two-step PCR method with two pairs of primers, 5′-GGGCCACAATGGAGCGGGGATGACGACCAC-3′ and 5′-CTGTCCCCCAGGACGTCCGCTTCATCCATG-3′ and 5′-GTGGTCGTCATCCCCGCTCCATTGTGGCCC-3′ and 5′-CTCAGTGGCTGTGATCATCAAGGGCATCG-3′. NBF2 Walker A lysine-1952 was substituted with methionine using a QuikChange site-directed mutagenesis kit (Stratagene) with a mutagenic primer, 5′-GGGGCTGGAATGTCATCAACTTTC-3′. The hMDR1 expression vector and recombinant virus were generated as described previously (6).

Generation of Recombinant Baculovirus—Recombinant baculovirus containing ABCA1-TATH (BV-ABCA1-TATH) was generated by the co-transfection of *Spodoptera frugiperda* 9 (Sf9) cells with pVL1392-ABCA1-TATH and Baculogold™ DNA. BV-ABCA1-TATH was purified and amplified following the manufacturer's directions. The generated virus was kept at 4 °C in the dark.

Expression of Human ABCA1 in Sf9 Cells—Sf9 cells were grown at 27 °C as a monolayer culture in Grace's insect medium (Invitrogen) with 10% fetal bovine serum or as a suspension culture in Grace's insect medium with 10% fetal bovine serum plus 0.1% purulonic F-68 (Invitrogen). Sf9 cells were infected with BV-hABCA1-TATH at a multiplicity of infection of 5. At 48 h after infection, cells were harvested and washed with ice-cold phosphate-buffered saline. Cells were stored at −80 °C.

Preparation of Microsomal Membrane—All the steps in the preparation of the microsomal membrane fraction were performed at 0–4 °C. Sf9 cells were thawed and resuspended in 10×cell volume of sonication buffer containing 20 mM Tris-HCl (pH 7.5), 10% (v/v) glycerol, 1 mM EDTA, and protease inhibitor mixture (100 μg/ml (*p*-amidinophenyl)-methanesulfonyl fluoride, 10 μg/ml leupeptin, and 2 μg/ml aprotinin). The cell suspension was sonicated for 5 min (output 5, 10 rounds of sonication for 30 s + interval of 2 min) with a probe tip-type sonicator (Misonix Inc.) and centrifuged at 3,000 × *g* for 10 min to remove unbroken cells and nuclei. The supernatant was centrifuged at 40,000 × *g* for 60 min. The microsome pellet was resuspended in ice-cold buffer A containing 50 mM Tris-HCl (pH 8.0), 50 mM NaCl, 30% (v/v) glycerol, 10 mM imidazole, 1 mM 2-mercaptoethanol, and protease inhibitor mix. The microsomal membrane suspension was passed through a 22-gauge syringe five times and stored at −80 °C. Micorosomal membrane protein (80–100 mg) was obtained from 10 g of wet cells.

Glycosylation Analysis—The reaction of *N*-glycosidase F (NGF) was performed as described previously (18). Lectin staining was performed as follows: After SDS-PAGE, proteins were transferred to a polyvinylidene difluoride membrane. The membrane was first blocked with block ACE (Dainihon Pharmaceutical) and incubated with 1 μg/ml of concanavalin A (Honen Corp.) in buffer containing 0.15 M NaCl, 0.01 M Tris-HCl (pH 7.5), and 0.05% Tween 20. The polyvinylidene difluoride membrane was then washed three times, and signals were detected with an ECL detection kit (Amersham Biosciences).

Extraction of ABCA1 from Sf9 Membrane—The microsomal membrane was resuspended with buffer A containing 0.6 or 0.8% *n*-dodecyl-β-D-maltoside (DDM) (Dojindo) and protease inhibitor mix and kept on ice with occasional gentle mixing for 30 min. The insoluble fraction was removed by centrifugation (100,000 × *g*, 60 min) in a TLA 100.4 rotor (Beckman).

Purification with Ni^{2+}-NTA-Agarose—All purification steps were performed at 0–4 °C. Extracted proteins were applied to Ni^{2+}-NTA-agarose (Qiagen) pre-equilibrated with buffer A. The mixture was rotated for 18 h. The resin was then washed with 20× bed volume of buffer A containing 0.1% DDM and 20 mM imidazole. ABCA1 or MDR1 was eluted with 2× bed volume of buffer A containing 0.1% DDM and 200 mM imidazole. The eluate was concentrated by ultrafiltration using a microcon YM-100 (Millipore) to 0.1–0.3 mg/ml protein. Protein concentrations were determined by the Bradford method using a protein assay kit (Bio-Rad) (19). Bovine serum albumin was used as a standard.

Purification with Anion Exchange Chromatography Sepharose, DE52—Proteins were mixed with pre-equilibrated DE52 Sepharose (Whatman) in DE52 binding buffer (50 mM Tris-HCl (pH 7.4), 30%(v/v) glycerol, 0.1% DDM, 1 mM 2-mercaptoethanol), and the mixture was rotated for 12 h. ABCA1 was eluted with DE52 binding buffer containing NaCl (50~200 mM) for 60 min. The flow-through fraction and eluate were concentrated by ultrafiltration using a microcon YM-100 to 0.1–0.2 mg/ml protein.

Cell Culture and Membrane Preparation—WI-38 human fibroblast cells and HEK293 stably expressing human ABCA1, generated by hygromycin selection as described previously (17), were grown at 37 °C in Dulbecco's modified Eagle's medium with 10% fetal bovine serum. WI-38 cells were seeded into a 100-mm dish at 5×10^6 cells. To induce ABCA1 expression, cells were cultured in the medium containing 10 μM TO901317 and 5 μM 9-*cis*-retinoic acid for 24 h. Crude membranes were prepared by nitrogen cavitation method as described previously (18).

Reconstitution of Purified ABCA1 with Lipids—L-α-Lecitin (20%) from soybean, sphingomyelin, or synthesized phospholipids dissolved in chloroform were dried by evaporation and resuspended in reaction buffer, 40 mM Tris-HCl (pH 7.5), 0.1 mM EGTA to a final concentration of 5 mg/ml. When sterols were incorporated into the liposomes, sterols were mixed with phospholipids in chloroform at first, then dried by

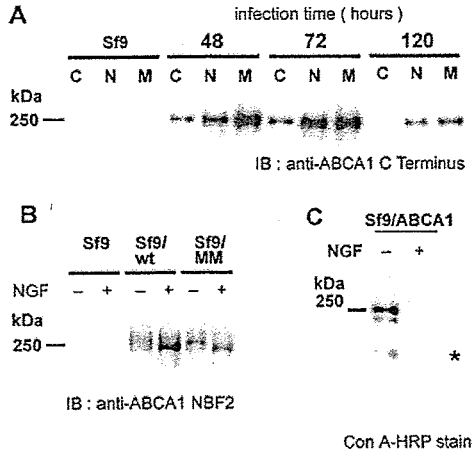

FIGURE 1. **Membrane localization and glycosylation of human ABCA1 expressed in Sf9 cells.** *A*, Western blotting of human ABCA1-TATH protein expressed in Sf9 cells. Proteins in cytosolic (*C*), nuclear (*N*), and microsomal (*M*) fractions (10 μg) were separated on 7% SDS-PAGE gel. ABCA1-TATH was detected with anti-ABCA1 terminus antibody. *B*, membranes prepared from Sf9 control cells or cells transfected with ABCA1-TATH, wild-type (*wt*), and mutant (MM) virus were treated with or without NGF. Proteins were separated on 7% SDS gel, and ABCA1-TATH was detected with anti-penta-His antibody. *C*, membranes prepared from Sf9 cells transfected with ABCA1-TATH virus were treated with or without NGF. Glycoproteins were detected with concanavalin A-conjugated horseradish peroxidase. A band marked by an *asterisk*, was also detected in Sf9 control cells (data not shown).

evaporation and resuspended in reaction buffer according to the standard procedure (20). The suspension was sonicated in a bath sonicator. To examine the effect of apoA-I, apoA-I (500 ng) was added to the suspension either before or after sonication. The lipid stock was stored at 4 °C under N_2 gas and kept in a dark place. Purified protein (100 ng) was mixed with 500 ng of lipid, and the mixture was incubated at 23 °C for 20 min. The reconstitution buffer for MDR1 contained 2 mM dithiothreitol.

Assay of ATPase Activity—Reactions were carried out in 16 μl of 40 mM Tris-HCl (pH 7.5), 0.1 mM EGTA, 10 mM Na_2ATP (pH 7.0), and 10 mM $MgCl_2$ at 37 °C for 30 min. Reactions were initiated by the addition of purified reconstituted ABCA1 (100 ng) and stopped by the addition of 14 μl of 12% SDS and vigorous mixing. ATPase activity was analyzed using two methods: (i) measuring released ADP by high performance liquid chromatography with titanium dioxide (21) and (ii) measuring released P_i by the P_i-Mo method (22, 23). The P_i released by the reaction with reconstituted ABCA1, predenatured by SDS, was subtracted as a negative control. Little or no ATP hydrolysis was observed in the reaction without protein.

RESULTS

Expression of Human ABCA1 in Insect Cells—We constructed a plasmid, pVL1392-ABCA1-TATH, to express human ABCA1 fused with a histidine tag and biotinylation tag at the C terminus, and this was introduced into insect Sf9 cells. Individual plaques were examined for the expression, and Sf9 cells were infected by the purified virus for large scale production and purification. Human ABCA1 expressed in Sf9 cells, about 250 kDa, was found most abundantly in the microsome membrane fraction in 48 h (Fig. 1*A*), and ABCA1 in the nuclear fraction increased in 72 h. The amount of ABCA1 decreased in 120 h probably due to degradation. Therefore, Sf9 cells were harvested at 48–72 h after infection. The amount of ABCA1 in the microsome membrane fraction accounted for about 1% of total membrane proteins.

Glycosylation of ABCA1 Expressed in the Sf9 Membrane—ABCA1 is glycosylated and has two large extracellular domains, which are suggested to be functionally important (24, 25). The glycosylation of ABCA1 expressed in Sf9 membranes was examined. The mobility of ABCA1, expressed in Sf9 membranes, in SDS-PAGE became faster by NGF treatment (Fig. 1, *B* and *C*). ABCA1 reacted with concanavalin A, which reacts mainly with high mannose-type sugar chains, but ABCA1 treated with NGF did not (Fig. 1*C*). These results suggest that human ABCA1 expressed in Sf9 is modified with high mannose-type sugar chains.

Solubility and Purification of ABCA1—As nonionic-detergent DDM was successfully used to solubilize recombinant ABC proteins (9, 26, 27), human ABCA1 expressed in the Sf9 membrane was extracted with 0.6% and 0.8% DDM (Fig. 2*A*). ABCA1, extracted with 0.6% and 0.8% DDM (*lanes 1* and *3*), migrated a little slower than it remained in the insoluble fraction (*lanes 2* and *4*). Roughly 50% of ABCA1 was extracted with DDM, and efficiency was not significantly increased even with 1.0% DDM (data not shown).

Extracted ABCA1 was purified using Ni^{2+}-NTA-agarose resin (Fig. 2*B*). ABCA1 was recovered from the resin with 200 mM imidazole (*lanes 10* and *11*) in 80–90% purity judged from Coomassie Brilliant Blue staining. Purity was not significantly different between 0.6 and 0.8% DDM extraction. About 100 μg of purified ABCA1 was obtained from 250 mg of microsome membranes of Sf9 cells cultured in 1L suspension culture.

Initially we planned to further purify ABCA1 with avidine column after *in vitro* biotinylation of the tag fused at the C terminus as reported previously (28); however, ABCA1 was not successfully recovered from the avidine column (data not shown). Therefore, we performed anion exchange chromatography using DE52 Sepharose (Fig. 2*C*). ABCA1, recovered from Ni^{2+}-NTA-agarose resin, was concentrated and mixed with pre-equilibrated DE52 Sepharose. The majority of ABCA1 did not bind to DE52 Sepharose, and ABCA1 could be purified as a flow-through fraction of DE52 (Fig. 2*C*). ABCA1 was recovered in almost pure form from DE52 Sepharose judging from Coomassie Brilliant Blue (Fig. 2*C*) and silver staining (Fig. 2*D*). ABCA1 K939M-K1952M protein, expressed and purified in the same procedure, was as pure as the wild type (Figs. 1*B* and 2*E*).

Trypsin Sensitivity of ABCA1—To confirm that purified ABCA1 retained the correct conformation after the purification procedure, we examined the trypsin sensitivity of ABCA1. ABCA1, endogenously expressed in human fibroblast WI-38 cells, was partially digested by trypsin. ABCA1 was partially cleaved to produce four fragments, 170 and 150 kDa and subsequently 125 and 110 kDa, which were recognized by anti-ABCA1 extracellular domain 1 antibody (KM3073) (Fig. 3*A*) and two fragments, 170 and 120 kDa, which were recognized by anti-ABCA1 NBF2 antibody (Fig. 3*B*). These fragments may be assigned to fragments digested at site A, just after the sixth transmembrane α-helix, and at site B, just before the seventh transmembrane α-helix as shown in Fig. 3*F*. It is predicted that the limited digestion at site A produces 150- and 110-kDa fragments and their glycosylated forms, and the limited digestion at site B produces 155- and 110-kDa fragments and their glycosylated forms as a diagram (Fig. 3*F*). When these fragments were analyzed by SDS-PAGE under non-reducing conditions, they co-migrated with undigested ABCA1 of about 280 kDa (supplemental Fig. 2). These results suggested that N and C halves of ABCA1 were connected with disulfide bonds.

When ABCA1 expressed in Sf9 cells was partially digested with trypsin, ABCA1 produced 140-kDa and subsequently 95-kDa fragments, which were recognized by KM3073 (Fig. 3*C*), and 155-kDa and subsequently 110-kDa fragments, which were recognized by anti-ABCA1 NBF2 antibody (Fig. 3*D*). All the produced fragments were smaller than

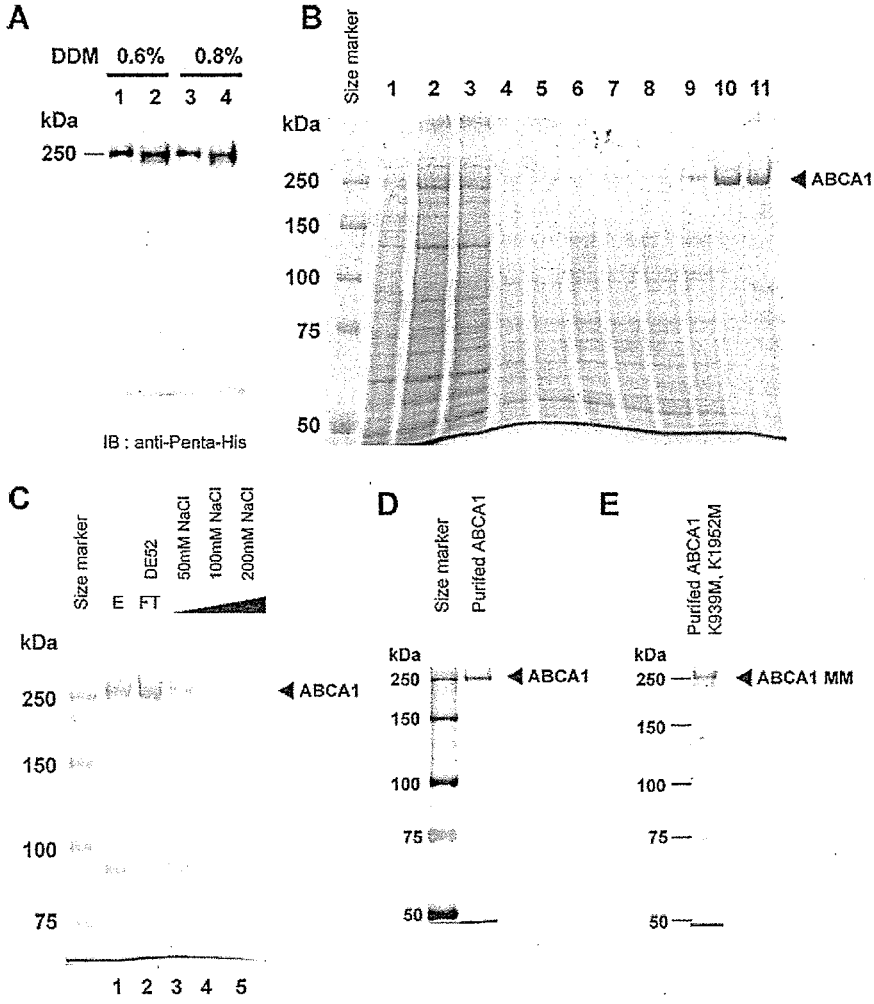

FIGURE 2. **Purification of ABCA1.** *A*, Sf9 membranes were extracted with 0.6% (*lanes 1* and *2*) and 0.8% DDM (*lanes 3* and *4*). *Lanes 1* and *3*, soluble fraction; *lanes 2* and *4*, insoluble fraction. Proteins (10 μg) were separated on 7% polyacrylamide gel, and ABCA1-TATH was detected with anti-penta-His antibody. *B*, Coomassie Brilliant Blue R-250 staining: *lane 1*, microsomes 10 μg; *lanes 2* and *3*, insoluble fraction after DDM extraction of microsomes 10 μg; *lanes 4* and *5*, soluble fraction after DDM extraction of microsomes 5 μg; *lanes 6* and *7*, flow-through from Ni^{2+}-NTA column, 5 μg; *lanes 8* and *9*, 20 mM imidazole eluate from Ni^{2+}-NTA column, 3 μg; *lanes 10* and *11*, eluate from Ni^{2+}-NTA column with 200 mM imidazole, 3 μg. *C*, Purification by DE52 column (Coomassie Brilliant Blue R-250 staining): *lane 1*, Ni^{2+}-NTA eluate; *lane 2*, DE52 flow-through fraction; *lane 3*, eluate from DE52 with DE52 binding buffer containing 50 mM NaCl; *lane 4*, eluate with buffer containing 100 mM NaCl; *lane 5*, eluate with buffer containing 200 mM NaCl. *D*, silver staining of DE52 flow-through fraction (25 ng). *E*, purified ABCA1 K939M-K1952M mutant, 0.5 μg (Coomassie Brilliant Blue R-250 staining).

the corresponding ones produced from ABCA1 of WI-38 cells probably due to glycosylation differences. When these fragments were analyzed by SDS-PAGE under non-reducing conditions, they co-migrated with undigested ABCA1 of about 250 kDa (supplemental Fig. 2). These results suggested that ABCA1 expressed in WI-38 cells and Sf9 cells contained similar typsin-sensitive sites (Fig. 3*E*).

Trypsin limited-digestion of purified detergent-soluble ABCA1, producing N-terminal 140- and 95-kDa fragments and C-terminal 155- and 110-kDa fragments (Fig. 3*E*). These fragments well corresponded to the fragments produced from ABCA1 endogenously expressed in WI-38 (Fig. 3, *A* and *B*), ABCA1 exogenously expressed in Sf9 cells (Fig. 3, *C* and *D*), and HEK293 cells (supplemental Fig. 1). These results suggest that purified ABCA1 retains conformation similar to ABCA1 endogenously expressed in human fibroblast membranes.

ATPase Activity of ABCA1—The ATPase activity of purified ABCA1 reconstituted in soybean lipids was examined. ATP was hydrolyzed by proteoliposomes in a time-dependent manner at 37 °C, and released phosphate ions increased linearly during 30 min (Fig. 4). Hence, the following ATPase assays were performed at 37 °C for 30 min in this study.

Next, we examined ATPase activity in the presence of various concentrations of MgATP. ATPase increased with increasing concentrations of ATP, and the apparent K_m for ATP and V_{max} were 112 μM and 455 nmol/min/mg of protein, respectively. The ATPase activity of purified reconstituted ABCA1 varied ranging from 400 to 900 nmol/min/mg of protein depending on preparations. Fig. 5 shows the representative data.

To confirm that ATPase activity is derived from purified ABCA1, a baculovirus for ABCA1 K939M-K1952M mutant, in which lysine 939 and lysine 1952 in the Walker A motif of nucleotide binding folds were replaced by methionines, was constructed. These lysines were reported to be indispensable for ATP hydrolysis of ABC proteins (29). Purified ABCA1 K939M-K1952M protein showed little ATPase activity, less than 10 nmol/min/mg of protein (Fig. 5). These results suggest that the purified ABCA1 reconstituted into soybean lipids shows ATPase activity.

Lipid Specificity in Stimulating ABCA1 ATPase—It has been reported that purified MDR1 shows ATPase activity only after reconstitution in liposomes and stimulation by transport substrates (30). We compared the ATPase activity of ABCA1 and MDR1 purified with the same procedure (Fig. 6*A*). Purified human MDR1 (supplemental Fig. 3) reconstituted in soybean lipids showed minimum ATPase activity, which was strongly stimulated only after the addition of verapamil, a transport substrate for MDR1. In contrast, ABCA1 showed significant ATPase activity even before reconstitution, and the ATPase activity was stimulated by the addition of soybean lipids. Verapamil did not affect the ATPase activity of ABCA1 either before or after reconstitution (data not shown).

We hypothesized that lipids themselves stimulate ABCA1 ATPase activity. If this is the case, we may speculate that there is lipid specificity

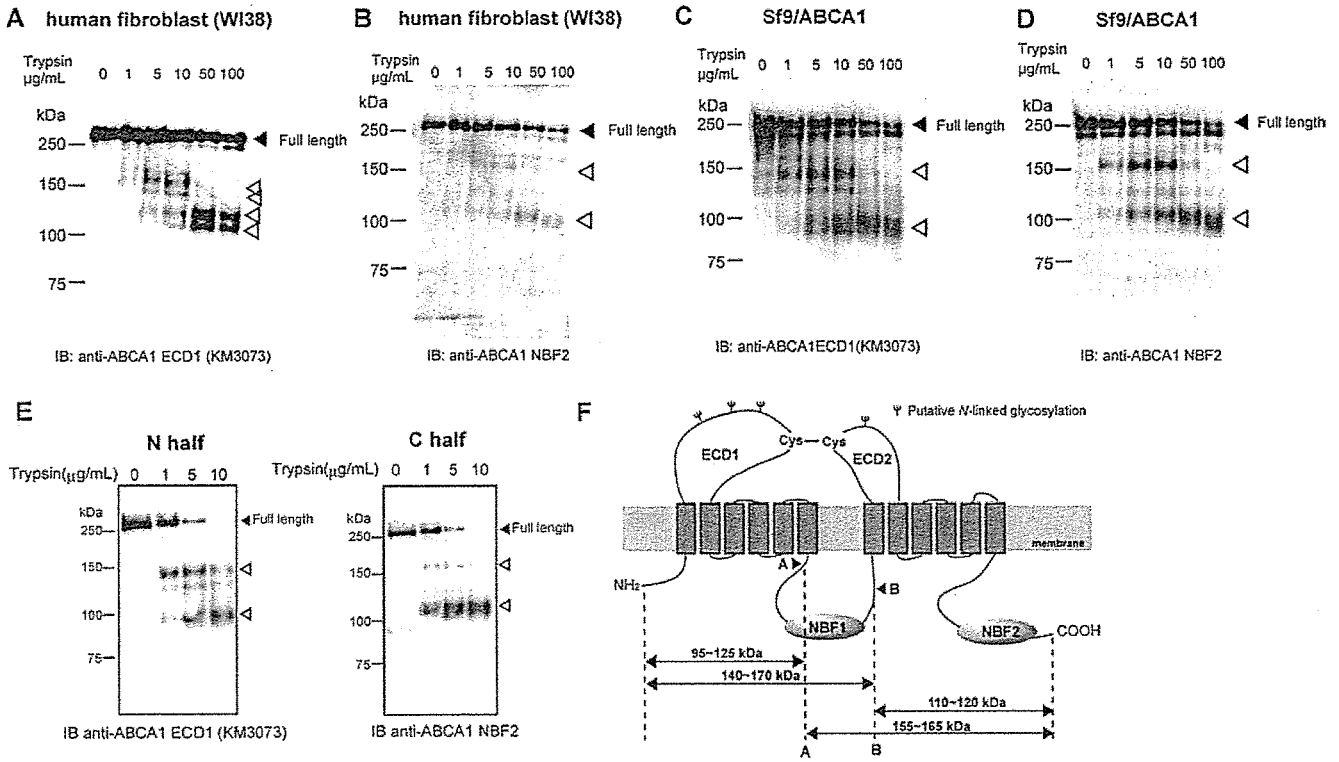

FIGURE 3. **Trypsin-limited digestion of ABCA1.** *A* and *B*, human fibroblast (WI-38) membranes treated with the represented concentration of trypsin were separated with 7% polyacrylamide gel under reducing conditions. ABCA1 was detected by anti-ABCA1 ECD1 monoclonal antibody (KM3073) (*A*) or anti-ABCA1 NBF2 polyclonal antibody (*B*). Full-length ABCA1 is indicated by a *black triangle* and limited digested ABCA1 fragments by *white triangles*. *C* and *D*, Sf9 membranes expressing ABCA1 were treated and detected as described above. *E*, purified ABCA1 was treated with 1, 5, and 10 μg/ml trypsin and detected as described above. *F*, schematic diagram of typsin-limited digestion of ABCA1 and the molecular size of produced fragments.

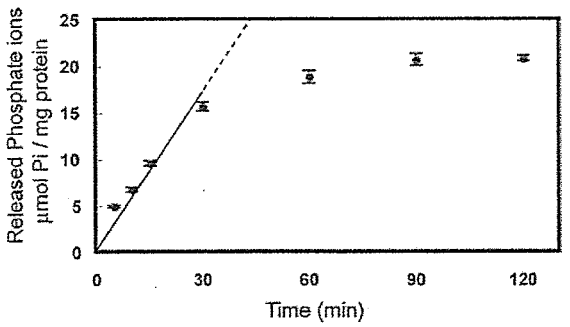

FIGURE 4. **Dependence of ATPase activity on the reaction time.** Purified ABCA1 was reconstituted with soybean lipids as described under "Experimental Procedures." Released inorganic phosphate ions were quantified. Each data point is the mean ± S.D. ($n = 4$).

in stimulating ABCA1 ATPase activity. To examine this possibility, we prepared liposomes composed of synthetic phospholipids with various head groups or acyl chains. ABCA1 was first reconstituted in liposomes composed of 16:0–18:1 PC and 16:0–18:1 PS in various ratios (Fig. 6*B*). ATPase activity was lowest when reconstituted in 100% PS liposomes, increased with the increasing ratio of PC, and was highest when liposomes contained more than 70% PC. In consequence, ABCA1 showed almost 2-fold higher ATPase activity in PC liposomes than in PS liposomes. Next, ABCA1 was reconstituted in liposomes composed of 16:0–18:1 PC and other phospholipid species such as SM, PE, or PG in various ratios (Fig. 6*C*). The content of SM in PC liposomes did not significantly affect the ATPase activity of ABCA1; however, PG inhibited the ATPase activity of ABCA1 depending on its content, and PE inhibited ATPase activity by 50%, even at 20% content (Fig. 6*C*). These results suggest that the ATPase activity of ABCA1 is stimulated preferentially by phospholipids with choline head groups, PC and SM. We also explored the preference of acyl chain length and the number of double bonds of phospholipids (Fig. 6*D*). When ABCA1 was reconstituted in liposomes containing PC (16:0–18:1), it showed higher ATPase activity than when reconstituted in liposomes containing PC (18:0–18:0), PC (20:0–20:0), or PC (18:0–18:1). These results suggest that there is some acyl chain preference in stimulating ABCA1 ATPase activity.

Effect of Sterols on ABCA1 ATPase Activity—As ABCA1 is involved in loading cellular free cholesterol onto apoA-I, we examined the effect of cholesterol and other sterols on ABCA1 ATPase activity. Purified ABCA1 was reconstituted in 16:0–18:1 PC and 16:0–18:1 PS (8:2) liposomes containing various amounts of cholesterol, and ABCA1 ATPase was analyzed. ABCA1 ATPase activity decreased in a dose-dependent manner of cholesterol and was reduced by 25% in the presence of 20% cholesterol (Fig. 7*A*). The structure specificity of sterols in inhibiting ABCA1 ATPase was examined. β-Sitosterol and campesterol showed a similar inhibitory effect with cholesterol (Fig. 7*B*). Brassicasterol and ergosterol showed intermediate effects, but stigmasterol scarcely inhibited ABCA1 ATPase.

Beryllium Fluoride and Glibenclamide Inhibit ABCA1 ATPase Activity—ABCA1 ATPase activity was completely abolished in the absence of magnesium ions (Fig. 8). It was also inhibited efficiently by beryllium fluoride, a phosphate analogue, but not by vanadate, another phosphate analog. Glibenclamide, which has been used as an inhibitor of ABCA1 in apoA-I-dependent cellular cholesterol efflux (3, 31, 32), suppressed the ATPase activity of ABCA1 in a dose-dependent manner,